ELSEVIER

Coordination Chemistry Reviews
156 (1996) 201–236

COORDINATION CHEMISTRY REVIEWS

Hydridotris(pyrazolyl)borato complexes of the Group 5 metals: inorganic and organometallic chemistry

Michel Etienne[1]

Laboratoire de Chimie de Coordination du CNRS, UPR 8241, 205 Route de Narbonne, F-31077 Toulouse Cedex, France

Received 10 July 1995; revised 31 October 1995

Contents

Abstract . . . 201
1. Introduction . . . 202
2. Vanadium . . . 203
   2.1. Vanadium complexes without the V=O moiety . . . 203
      2.1.1. Vanadium(II) . . . 203
      2.1.2. Vanadium(III) . . . 204
      2.1.3. Vanadium(IV) and (V) . . . 205
   2.2. Vanandium complexes with the V=O moiety . . . 206
      2.2.1. Vanadium(IV) . . . 207
      2.2.2. Vanadium(V) . . . 211
      2.2.3. Carboxylato-bridged vanadium complexes . . . 213
3. Niobium and tantalum . . . 215
   3.1. Niobium and tantalum(IV) and (V) . . . 215
   3.2. Niobium(III) . . . 219
      3.2.1. Dichloro(alkyne) complexes and alkyne alkylation reactions . . . 219
      3.2.2. Hydrocarbyl derivatives . . . 224
      3.2.3. Alkyne coupling reactions . . . 228
4. Recent work and conclusions . . . 230
Note added during revision . . . 233
Acknowledgements . . . 234
References . . . 234

Abstract

This review is devoted to the inorganic and organometallic chemistry of Group 5 metal complexes containing hydridotris(pyrazolyl)borates. The first part of the review describes the

[1] E-mail: etienne@lcctoul.lcc-toulouse.fr

SSDI 0010-8545(95)01236-2

advances made in the chemistry of tris(pyrazolyl)borato vanadium complexes. The physicochemical properties of these complexes are being studied mainly to model vanadium–histidine interactions which occur in metalloproteins such as bromoperoxidase. Although most of the complexes studied to date are oxo vanadium species, some other simple hydridotris(pyrazolyl)borato vanadium complexes have also been synthesized, but their organometallic chemistry remains undeveloped. The second part of the review focuses on the organometallic chemistry of hydridotris(pyrazolyl)borato niobium and tantalum complexes. The main advances have been made in the field of four-electron alkyne niobium complexes. The structural data available are described and, as far as possible, correlated with the observed organometallic chemistry. Throughout, comparison with known Group 5 alkyne and related (such as imido, etc.) complexes containing cyclopentadienyl ligands is emphasized. Although very few articles have yet appeared, the results indicate clearly that a rich and promising organometallic chemistry can be expected.

Keywords: Group 5; Hydridotris(pyrazolyl)borato compounds

1. Introduction

Although the coordination chemistry based on poly(pyrazolyl)borato ligands has been reviewed in comprehensive texts [1], chiefly by Trofimenko who discovered them, this shorter review devoted to the chemistry of the Group 5 metals (V, Nb, Ta) has clear purposes. The most important one is that, since the last review which appeared in 1993, poly(pyrazolyl)borate chemistry of the Group 5 metals, and particularly that of niobium, which was clearly underdeveloped, has started to blossom. In addition to the previous comprehensive reviews, shorter texts describing in more depth some particular areas and applications of the chemistry are valuable [2]. The chemistry of the Group 5 metal complexes also serves to illustrate nicely fundamental and widespread aspects of the utilization of poly(pyrazolyl)borato ligands. One aspect is bioinorganic chemistry where the tris(pyrazolyl)borato complexes are used as models probing the histidine(imidazole)–metal interactions in several types of metalloproteins. These ideas have given the main impetus to the vanadium chemistry which is presented in the first section of the review. The second aspect has found most of its applications in organometallic chemistry, where the tris(pyrazolyl)borates are used as alternatives to the cyclopentadienyl ligands. This aspect is particularly dealt with in the second main section of the review describing the chemistry of niobium and tantalum complexes.

We will follow the nomenclature used by Trofimenko [1b]. Hence the abbreviations Tp, Tp* and pzTp stand for unsubstituted hydridotris(pyrazolyl)borate, hydridotris(3,5-dimethylpyrazolyl)borate and tetrakis(pyrazolyl)borate, respectively. These are the only ligands which have as yet given stable complexes of the Group 5 metals, with the Tp and Tp* complexes being by far the more common. Other ligands of the family have been used in some instances, but with less success. These monoanionic ligands are formally six-electron donors with C_{3v} symmetry which will coordinate to a metal via the nitrogen atoms in the 2-position. The shape of the poly(pyrazolyl)borates is particularly well suited to the octahedral coordination. Three facial sites of coordination will tend to be occupied leaving the three

other cis sites available for other ligands and chemistry. Tp and Tp* have different stereoelectronic properties, and this will be illustrated in the review.

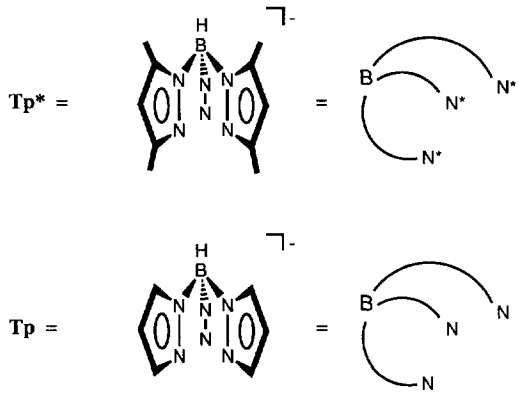

2. Vanadium

Vanadium tris(pyrazolyl)borato complexes have been described for oxidation states between II and V, with the chemistry of vanadium(II) being by far the least developed. An important aim of the vanadium chemistry is to model vanadium–histidine interactions thought to be present in the enzyme bromoperoxidase. In these studies, the V=O unit is ubiquitous. Hence, for the sake of clarity and homogeneity, complexes that do not exhibit the oxo functionality are described first, while those with the V=O unit follow. All of the carboxylato-bridged complexes, containing either V=O or V–O–V units, are described in this latter section.

2.1. Vanadium complexes without the V=O moiety

2.1.1. Vanadium(II)

The first vanadium complexes (oxidation states II and III) containing hydridotris(pyrazolyl)borate were synthesized in 1975, with the aim of comparing its ligating properties with those of the cyclopentadienyl fragment [3]. The sublimable TpCpV is isolated as a green crystalline material in 47% yield from a mixture of products following the reaction of Cp_2VCl and KTp in THF. Obviously the mechanism is unclear, with both reduction of the vanadium and ligand exchange being involved. TpCpV is paramagnetic, with $\mu_{eff}=3.59\ \mu_B$, and it absorbs visible light at 688 nm ($\varepsilon=102\ l\ mol^{-1}\ cm^{-1}$) in THF. As compared to isoelectronic Cp_2V, TpCpV is only slowly air-oxidized [3]. The analogous compound Tp_2V has been synthesized via reaction of VBr_2 with two equivalents of KTp in hot ethanol [4]. No yield is reported for this reaction. The value of the magnetic moment ($\mu_{eff}=3.82\ \mu_B$) and the electronic spectrum (dichloromethane, 541 (100), 422 (sh), 385 (5450), 351 (sh), 270 (sh), 250 (7150) nm) are consistent with a high-spin, d^3 octahedral configuration. Surprisingly, there is no report describing the analogous Tp^*_2V.

2.1.2. Vanadium(III)

The coordination chemistry of this oxidation state is more extensive, and several of the products that are described have served, or may serve, as useful starting materials for further developments. In these syntheses, vanadium trichloride VCl_3, either complexed or not, is the metal reagent of choice.

The first synthesis (1975) involved reaction of $VCl_3(THF)_3$ with KTp in THF to give the sparingly soluble green complex $TpVCl_2(THF)$ (**1**) in 92% yield [3]. Physicochemical properties are in accord with an octahedral high-spin d^2 configuration. Surprisingly, despite the ease and the high yield of its preparation, no chemistry has been described with this complex. Furthermore, most of the syntheses reported subsequently (except the one which is described directly below), suffer from extensive decomposition, resulting in low yields.

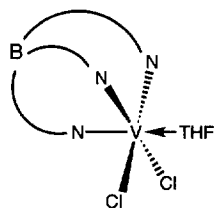

1

Green $TpVCl_2(DMF)$ and $Tp^*VCl_2(DMF)$ are obtained on a 5 g scale from VCl_3 and either KTp or KTp* in DMF in 58% yield [5]. $Tp^*VCl_2(DMF)$ was reported earlier by the same authors and found to crystallize from a variety of solvents [6]. Purple $Tp^*VCl_2(DMF)(H_2O)$, analytically characterized, is suggested to contain a bidentate Tp* with one dangling pyrazole arm, the vanadium(III) being six-coordinate overall. However, upon crystallization from benzene, the green complex $Tp^*VCl_2(DMF)$ (**2**) is obtained as the benzene solvate. Its structure has been determined by X-ray diffraction. Physicochemical data are consistent with the observed distorted octahedral coordination, the Tp* being tridentate. Brief mention is made of the hydridotris(3-phenylpyrazolyl)borato and hydridotris(3-*tert*-butylpyrazolyl)borato analogs [6].

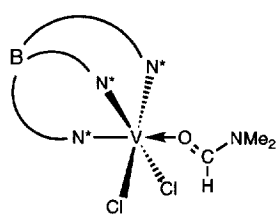

2

When the reactions between VCl_3 and KTp* are carried out in less basic solvents such as dichloromethane and THF, complex mixtures of products are formed, with obvious degradation of the Tp*, presumably via acid cleavage of the B–N bond.

This decomposition pathway is noted in several other instances and particularly in the Group 5 chemistry (see below). The ionic vanadium(III) complex $K[Tp^*VCl_2(Me_2pz)]$ is structurally characterized with further oxidation leading to the dinuclear species $[VOCl_2(Me_2pz)_2]_2.THF$, also characterized by X-ray analysis [6]. A similar decomposition is observed upon mixing VCl_3 and $K[HB(3\text{-}^tBupz)_3]$ in acetonitrile and exposure to air [7].

Attempted selective synthesis of methoxo complexes from these DMF complexes proved unsuccessful. Upon mixing $Tp^*VCl_2(DMF)$ with sodium methoxide in toluene, a mixture of the mono- and di-methoxo complexes is obtained [8]. Crystals were hand-separated and the X-ray crystal structure of Tp*VCl(OMe)(DMF) (**3**) determined. The molecule contains a short V–OMe bond (1.829(4) Å), compared with the V–O bond (2.086(3) Å) between the vanadium and the DMF. In $Tp^*VCl_2(DMF).C_6H_6$ the vanadium–oxygen distance is 2.082(5) Å [6]. The vanadium–methoxo-oxygen bond length is also less than the sum of the covalent single-bond radii of vanadium and oxygen, suggesting multiple-bond character for this interaction, consistent with the π-donating properties of alkoxo ligands [8]. Typical vanadium–oxygen double bonds are in the range 1.59–1.63 Å; see Section 2.2.

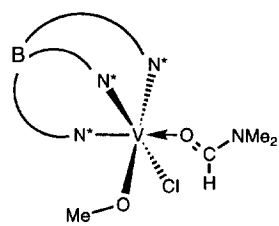

3

The last type of vanadium(III) compound currently known is the analog of the vanadocenium cation. Both $[Tp_2V][BPh_4]$ and $[Tp^*_2V][BPh_4]$ are prepared from VCl_3 and KTp or KTp* in hot acetonitrile [5]. Yields exceed 60%. The crystal structures of $[Tp_2V][BPh_4]$ and $[Tp^*_2V][OMe]$ have been determined. Slightly distorted octahedral coordination is observed, with virtually identical bond lengths in the two cases, indicating little steric interaction, as observed elsewhere (see Section 2.2). The V–N bond lengths range from 2.055(2) to 2.095(2) Å, averaging 2.079(2) Å in the two independent molecules of $[Tp_2V][BPh_4]$, whereas for [Tp*V][OMe] the average V–N bond length is 2.083 Å [5]. These V^{III} cations cannot be oxidized at potentials up to 2.0 V. One-electron reduction forms reversibly the corresponding stable V^{II} complexes. As expected, the methyl-substituted $[Tp^*_2V][BPh_4]$ is more difficult to reduce than $[Tp_2V][BPh_4]$ ($E^\circ = -0.69$ V and -0.42 V, respectively). The high stability of the V^{III} and V^{II} oxidation states is attributed to the sandwich structure which encapsulates the metal. Note that Tp_2V has been prepared previously [4] (see Section 2.1.1).

2.1.3. Vanadium(IV) and (V)

To our knowledge, excluding oxo complexes, there is only one example described to date for each of these two oxidation states.

The dark purple-brown vanadium(IV) complex $TpVCl_3$ is obtained in 38% yield after mixing VCl_4 and KTp in dichloromethane. Only limited analytical data are reported. The compound is rapidly decomposed by air oxidation and hydrolysis [9].

In oxidation state V, the recently described reaction of $VCl_3(N\text{-}^tBu)$ with KTp* in THF yields green $Tp^*V(N\text{-}t\text{-}Bu)Cl_2$ (**4**) in 56% yield [10]. The niobium and tantalum analogs are reported (see Section 3.1) as well as other oxo- and *tert*-butylimido complexes of Groups 6 and 7 with Tp* as a coligand. An IR absorption band at 1207 cm^{-1} is assigned to the V=N–C vibration. A more detailed discussion of imido complexes is provided in Section 3.1. No chemistry starting from $Tp^*V(N\text{-}t\text{-}Bu)Cl_2$ has been described (see however Section 4).

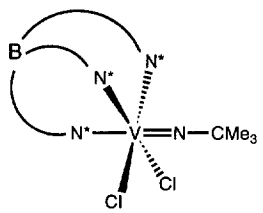

4

2.2. *Vanadium complexes with the V=O moiety*

As briefly stated in the introduction, the studies of complexes containing the V=O moiety are related largely to modeling histidine–vanadium interactions that could be present in enzymes such as bromoperoxidase (V-BrPO). The occurence of vanadium in living systems and the relevant chemistry have been reviewed [11–13]. A paper specifically reviewing marine haloperoxidases has appeared recently [14].

V-BrPO is a vanadium(V)-dependent enzyme found in marine algae. It catalyzes reaction (1):

$$RH + H_2O_2 + Br^- \rightarrow RBr + H_2O + OH^- \quad (1)$$

A model has been proposed for the vanadium environment in the enzyme based on several physicochemical techniques such as EPR, EXAFS, UV–vis and ^{51}V NMR spectroscopies. V-BrPO exhibits a high-field ^{51}V NMR chemical shift [15], partially consistent with η^2-ligands such as glutamate or aspartate [16]. A vanadate-dependent shoulder around 315 nm is present in the UV–vis absorption spectrum of the enzyme [17]. From EXAFS studies [18], the vanadium(V) may be in a distorted octahedral coordination geometry with three unidentified light-atom donors (probably oxygen or nitrogen) at 1.72 Å, two nitrogen donors at 2.11 Å, almost certainly from histidine (imidazole) nitrogens, and a single terminal oxo group at 1.61 Å. In the inactive, reduced enzyme, which would be in a similar environment, the main difference is a lengthening of the vanadium–light atom bond length to 1.91 Å. The reduced enzyme gives a pH-dependent anisotropic axial EPR spectrum, consistent with nitrogen/oxygen ligation [19]. Accordingly, water or hydroxide have

been proposed as ligands, but aspartate and glutamate are also good candidates, as well as alkoxo ligands from deprotonated serine or threonine.

Following these guidelines, the tris(pyrazolyl)borates, among several other species [11,12], have been utilized to build models whose physicochemical studies might lead to a better understanding of the coordination of the vanadium in V-BrPO. The groups of Collison and Mabbs and of Carrano have used this approach extensively. As usual, subsections are given for each oxidation state of the metal, *e.g.* IV and V. Carboxylato-bridged dimers are described separately.

2.2.1. Vanadium(IV)

Two general approaches have been followed for the synthesis of oxovanadium(IV) species. One involves the oxidation of a non-oxo tris(pyrazolyl)boratovanadium(III) complex and the other one utilizes a preformed oxovanadium(IV) complex to which the tris(pyrazolyl)borate is added by metathesis.

The simple vanadyl complexes (η^2-Tp*H)$VOCl_2$ [6], Tp*VO(Cl)(DMF) [6], and TpVO(Cl)(DMF) [5] have been obtained by the first method. As stated in Section 2.1.2, the reaction of VCl_3 with KTp*, leading to the corresponding Tp^*V^{III} complex, is highly solvent-dependent. Similarly, when these reaction mixtures are exposed to the air, different products are obtained, depending on the solvent. From THF, a peculiar V^{IV} complex (η^2-Tp*H)$VOCl_2$ (**5**) is isolated in low, unspecified yield [5]. According to X-ray crystallography, the complex contains a five-coordinate vanadium and a bidentate Tp*H with one dangling protonated pyrazole ring. The vanadium is then in a square-pyramidal environment. The compound is markedly different from the octahedral oxo–niobium(V) and oxo–tantalum(V) complexes Tp^*MOCl_2 reported more recently (see Section 3.1) [10]. From DMF in air, TpVO(Cl)DMF [5] and Tp*VO(Cl)DMF [6] are isolated in 61% and 30% yield, respectively, and fully characterized.

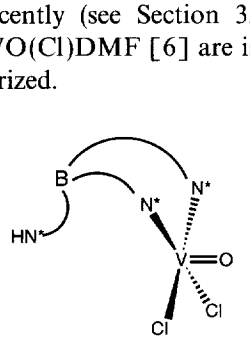

5

The second approach has been used to synthesize Tp*VO(Cl)(Me_2pzH) from KTp* and $VOCl_2(MeCN)_2(H_2O)$ [20]. The low yield (20–30%) and the presence of bound dimethylpyrazole are obviously due to some decomposition of the Tp* via B–N bond cleavage, a reaction observed in other instances. Addition of silver benzoate via a metathesis reaction leads to the η^1-benzoato-complex Tp*VO(η^1-O_2CPh)(Me_2pzH). This constitutes one of the rare reactivity studies on the basic

complexes [20]. From sodium malonate, a bridged dimer is obtained, whose description is to be found in Section 2.2.3.

Chelated complexes in the β-diketonate series are also synthesized, starting from VO(β-diketonato)$_2$ and KTp or KTp*. TpVO(acac) is obtained in 55% yield from methanol [5,6]. Independently, six different β-diketonato complexes, including Tp*VO(acac), are isolated from toluene reaction mixtures [21,22]. Dithiocarbamato complexes are also known [23,24], although in this case no full paper has appeared.

Selected geometric parameters derived from X-ray crystal structures are provided in Table 1. Tp*VO(Cl)(DMF) (**6**) shows a distorted octahedral geometry for the vanadium(IV). The oxo–vanadium bond length is 1.649(5) Å, consistent with a

Table 1
Selected bond distances (Å) from X-ray diffraction analyses of pseudo-octahedral TpVO compounds

Compound	V=O	V–O	V–N[a]	Ref.
Vanadium(IV)				
Tp*VO(Cl)(DMF)	1.649(5)	2.043(4)	2.329(6) 2.110(5) 2.117(5)	[6]
Tp*VO(η^1-O_2CPh)(Me_2pzH)	1.590(8)	1.996(6)	2.285(8) 2.106(7) 2.105(7)	[20]
Tp*VO(Cl)(Me_2pzH)	1.599(4)	—	2.355(4) 2.107(6) 2.107(4)	[20]
Tp*VO(acac)	1.596(2)	2.004(1) 2.013(1)	2.328(2) 2.111(2) 2.120(2)	[21]
TpVO(acac)	—[b]	—[b]	—[b]	[5]
Tp*VO(S_2CNPr_2)	1.589(4)	2.442(2)[c] 2.459(2)[c]	2.458(4) 2.108(4) 2.092(5)	[24]
Vanadium(V)				
Tp*VO(O-p-$C_6H_4Br)_2$	1.579(4)	1.822(4) 1.857(4)	2.311(5) 2.119(5) 2.088(5)	[25]
TpVO(Cl)(O-*i*-Pr)	1.587(5)	1.719(4)	2.259(5) 2.142(6) 2.090(5)	[8]
TpVO(Cl)(O-*t*-Bu)	1.631(3)	1.726(3)	2.274(4) 2.153(4) 2.106(4)	[8]
Tp*VO(Cl)(O-*t*-Bu)	1.592(8)	1.754(7)	2.313(9) 2.231(9) 2.116(9)	[8]

[a] N from hydridotris(pyrazolyl)borato.
[b] Data not provided [5], reported to be close to those for Tp*V(O)(acac) [21].
[c] V–S bond lengths.

somewhat long double bond. The dative bonding between the vanadium and the DMF leads to a V–O bond length of 2.043(4) Å [6]. In the η^1-benzoato complex Tp*VO(η^1-O_2CPh)(Me_2pzH) (**7**), the vanadium–*O*–carboxylato "single" bond length is 1.996(6) Å and the V=O bond length is 1.590(8) Å. In Tp*VO(Cl)(Me_2pzH) (**8**), a V=O bond length of 1.599(4) Å is observed [20]. These compounds thus provide an opportunity to compare different vanadium(IV)–oxygen bond types in closely related systems. Vanadium(V)–oxygen bond lengths are compared in the next section. In all of these structures the Tp* is η^3-bound to the vanadium with the V–N bond trans to the oxo group markedly longer than the two other V–N bonds, whatever the other ligands. This illustrates the strong trans influence of the oxo ligand.

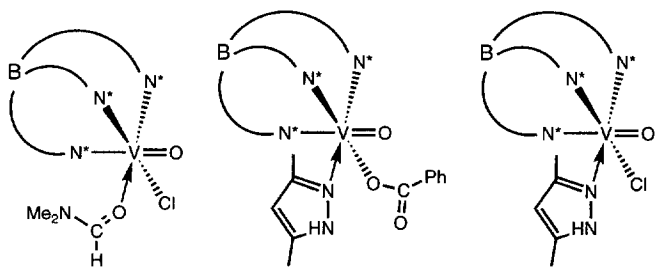

6 **7** **8**

Virtually all of the complexes reported have also been characterized by a number of different techniques. The data are consistent with pseudooctahedral d^1 vanadium(IV) structures. Detailed studies of molar conductance, magnetic properties, UV–vis, IR, EPR and X-ray diffraction data on the Tp and Tp* complexes (see Tables 1 and 2) indicate that, in general, the methyl groups in the Tp* ligand have the expected modest electron-releasing effect, but that they have only a small, if any, influence attributable to increased steric demand [5]. The cases of the chloro(DMF) and acac complexes are typical, and some relevant physicochemical data reported in Table 2. Perhaps the most interesting phenomena can be observed in the electrochemical behavior of these pairs of complexes. They all show quasi-reversible one-electron oxidations on the cyclic voltammetry time scale ($v = 200$ mV s^{-1}). As may be expected from the electron-releasing properties of the methyl groups, the oxidation of Tp* complexes occurs at less positive potentials. However, as pointed out [5], the main difference resides in the kinetic stability of the oxidized species. The bulk oxidation of the acac complexes only gives a moderately stable, deep blue oxovanadium(V) complex with Tp* as the ligand [5,25]. Similar behavior is observed for the non-chelated TpVO(Cl)(DMF) and Tp*VO(Cl)(DMF). Bulk oxidation of Tp*VO(Cl)(DMF) generates a deep blue oxovanadium(V) complex ($\lambda_{max} = 570$ nm, $\varepsilon = 1200$ l mol^{-1} cm^{-1}), whose cyclic voltammogram is identical to that of the starting material. This suggests the starting vanadium(IV) complex is very similar in structure to the vanadium(V) species. The rapid reduction of this oxidized species regenerates the original vanadium(IV) complex. The oxidized unsubstituted Tp

Table 2
Physicochemical data of some mononuclear pseudo-octahedral $TpV^{IV}O$ compounds

Compound	IR[a]	UV−vis[b]	CV[c]	EPR[d]	Ref.
TpVO(Cl)(DMF)	–	710 (55) 571 (42) 452 (sh, 32)	1.33	1.972 (99.9)	[5]
Tp*VO(Cl)(DMF)	965	762 (48) 589 (27) 390 (sh, 47)	1.21	1.971 (100.3)	[5,6]
TpVO(acac)	–	750 (36) 541 (17) 394 (sh, 43)	1.21	1.972 (100.0)	[5]
Tp*VO(acac)	957	775 (56) 560 (13) 402 (51)	1.07 1.11[e]	1.971 (101.1)	[5]
	963	763 (54)[f] 568 (11) 413 (50) 398 (50) 313 (8680)	1.14[e]	1.972 (98.9)[f]	[21]

[a] KBr, ν(V=O), cm^{-1}.
[b] CH_2Cl_2, λ, nm (ε, $l\,mol^{-1}\,cm^{-1}$).
[c] CH_2Cl_2, quasi-reversible processes, E^0 (V vs. SCE).
[d] CH_2Cl_2, principal or isotropic g (A, Gauss).
[e] In MeCN.
[f] In toluene.

complex directly gives yellow decomposition products thought to be dimers with both terminal and bridged oxo ligands [5]. Thus, the bulky Tp* ligand clearly shields the metal more efficiently than Tp itself, providing a higher kinetic stability to the complexes. Recall here that Tp* has a cone angle of 224°, whereas that of Tp is 184° [26]. The authors emphasize the observation of the highly colored vanadium(V) complex $[Tp^*VO(Cl)(DMF)]^+$ [5]. This LMCT transition is obviously due to the chloro ligand acting as a π-donor. Halide ions might be expected to bind to vanadium(V) during the catalytic cycle involving V-BrPO [14].

The family of Tp*(β-diketonato) complexes has been the subject of detailed spectroscopic studies [21–23]. As judged from X-ray crystal structures, there are virtually no differences between Tp*VO(acac) (**9**) [21] and TpVO(acac) [5] (Table 1). Both the electronic and EPR spectra reflect the low symmetry of the complexes (Table 2). The observation of four d–d bands on the one hand and rhombic EPR symmetry on the other is consistent with either a distorted D_{3d} or a C_s symmetry [21]. Single-crystal EPR studies on these and related dithiocarbamato complexes have been described briefly [22,23], but no full paper has been published. The crystal structure of $Tp^*VO(S_2CNPr_2)$ (**10**) also shows approximate C_s symmetry [24], with a V=O bond length the same as that in Tp*V(O)(acac).

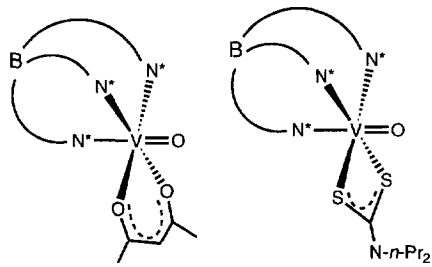

9 **10**

The η^1-benzoato and chloro complexes Tp*VO(η^1-O_2CPh)(Me_2pzH) and Tp*VO(Cl)(Me_2pzH) have also been characterized spectroscopically (electronic spectra and simulated X- and Q-band EPR spectra). Cyclic voltammetry indicates reversible one-electron oxidation ($v = 200$ mV s^{-1}), with that of the η^1-benzoato complex being 200 mV less positive than that of the chloro complex, consistent with the better π-donating properties of the former [20]. As far as modeling of V-BrPO is concerned (see Introduction), the V–O bond length of 1.996(6) Å observed for the vanadium(IV)–η^1-O_2CPh bond compares reasonably well with the 1.91 Å bond length between the vanadium center and the "light atom" in the reduced form of the enzyme. However, Tp*(carboxylato) complexes in the oxidation state V, which could serve as more accurate models, are lacking.

2.2.2. Vanadium(V)

The known stable oxo vanadium(V) complexes are all neutral, with alkoxo or phenoxo ligands. Their syntheses involve either oxidation of Tp or Tp* vanadium(IV) alkoxo complexes or preparation of oxovanadium(V) alkoxo species prior to addition of Tp or Tp*.

A series of *para*-substituted phenoxo complexes has been prepared in 30% yield from Tp*VO(Cl)(DMF) and the appropriate phenoxide salt followed by air-oxidation, according to Eq. (2) [25].

$$\text{Tp*VO(Cl)(DMF)} + 2\text{NaO-4-C}_6\text{H}_4\text{X} \xrightarrow[\text{toluene}]{\text{O}_2} \text{Tp*VO(O-4-C}_6\text{H}_4\text{X})_2 + \text{NaCl} + \text{DMF} \quad (2)$$

where X is H, Me, *t*-Bu, Br, NO_2.

Monoalkoxo complexes have been obtained in 75% yield according to the second procedure depicted in Eq. (3) [8].

$$\text{VOCl}_3 + \text{HOR} \xrightarrow{\text{pentane}} \text{VOCl}_2\text{(OR)} \xrightarrow{\text{KTp}} \text{TpVO(Cl)(OR)} \quad (3)$$

where R is Me, Et, Pr, *t*-Bu.

The bis(isopropoxo) complex TpVO(O-*i*-Pr)$_2$ is formed from KTp and VO(O-*i*-Pr)$_3$. There is extensive decomposition when starting from the oxychloride compound [8].

With Tp*, the bis(alkoxo) derivatives are isolated only with R as Me or Et, presumably because of the bulk of the other alkoxo ligands. The synthetic approach in this case involves the preparation of vanadium(IV) alkoxo complexes followed by oxidation with a silver salt and deprotonation with a non-nucleophilic base; see Eq. (4). Typical yields are 30% [8].

$$Tp^*VO(Cl)(DMF) + AgNO_3 \xrightarrow{ROH,DBU} Tp^*VO(OR)_2 + AgCl \quad (4)$$

As noted above, Tp* as compared to Tp gives these complexes a higher kinetic stability. The Tp complexes are readily hydrolyzed to give oxo-bridged species. The X-ray crystal structure of the tetramer $[TpVO_2]_4$ has been determined [8].

In the ^1H NMR spectra of the bis(alkoxo) and bis(phenoxo) complexes, the 1:2 intensity pattern for each type of Tp or Tp* protons indicates the presence of a plane of symmetry. The X-ray structures of several derivatives (**11**, **12**) have been obtained, and relevant metrical parameters are compiled in Table 1. An important feature of these molecular structures is that the vanadium–alkoxo-oxygen bonds are only 0.10–0.15 Å longer than the vanadium–oxo double bonds. This is attributed to the high π-donor character of the alkoxo ligand. The average length of vanadium–phenoxo-oxygen bonds is 1.84 Å, 0.1 Å longer than vanadium–alkoxo-oxygen bonds. There are small differences in bond lengths between TpVOCl(O-*t*-Bu) and Tp*VOCl(O-*t*-Bu). As for vanadium(IV) complexes, the oxo group exerts a strong *trans* influence, lengthening the vanadium–nitrogen bond *trans* to it. Finally, as generally observed, the vanadium–oxo bond length is virtually independent of the oxidation state IV or V in these complexes.

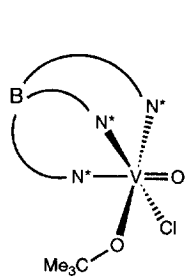

11

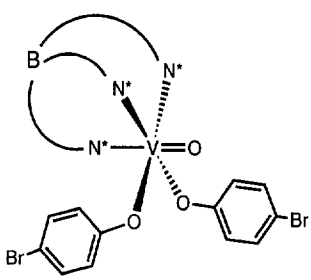

12

These complexes have also been studied by means of UV–vis absorption spectroscopy, cyclic voltammetry, ^{51}V NMR spectroscopy and, for some of them, EXAFS. The deep green to dark blue phenoxo complexes exhibit three absorption bands in their optical spectra, with molar extinction coefficients in the range 4000–8000 l mol^{-1} cm^{-1}. A blue-shift of the lowest energy band is observed as the electron-withdrawing power of the para-substituent increases, indicating a phenoxo-based LMCT. A plot of λ_{max} vs. Hammet σ constants is linear, the two extremes being the 4-methoxo ($\lambda_{max} = 800$ nm, $\varepsilon = 4540$ l mol^{-1} cm^{-1}) and the 4-nitro complexes ($\lambda_{max} = 630$ nm, ε 8750 l mol^{-1} cm^{-1}) [25]. A similar trend is observed for the

quasi-reversible one-electron reduction of these complexes. The 4-nitrophenoxo is the easiest to reduce ($E^\circ = 0.510$ V) and 4-methoxide substitution shifts the redox process to a more negative value by about 600 mV ($E^\circ = -0.125$ V) [25]. The alkoxo complexes are red to yellow, with low-intensity transitions in the blue region of the visible spectrum. The lowest energy band around 400 nm is attributed to a LMCT transition ($\varepsilon = 450$–2000 l mol^{-1} cm^{-1}) involving a pπ orbital on the alkoxide oxygen. The transition for dialkoxo complexes occurs at higher energy than for monoalkoxo complexes [8].

The ^{51}V NMR spectra yield no unusual chemical shifts due to alkoxo or phenoxo coordination. The chemical shifts are in the range δ −484 to δ −588, with Tp*VO(O-4-$C_6H_4OMe)_2$ and Tp*VO(O-4-$C_6H_4NO_2)_2$, respectively, as the two extremes [8,25]. Tp*VO(Cl)(O-*t*-Bu) and TpVO(Cl)(O-*t*-Bu) give resonances at δ −559 and δ −572, respectively. Controlled hydrolysis of several alkoxo derivatives gives a species tentatively described as the bis(hydroxo) complex Tp*VO$(OH)_2$. It gives a signal at δ −580 [8]. The tetramer $[TpVO_2]_4$ gives a resonance at δ −694. Typical chemical shifts and trends for vanadium(V) oxo species have been compiled and analyzed [27].

EXAFS data for Tp*VO$(OMe)_2$ and Tp*VO(O-4-$C_6H_4Br)_2$ are reported [8], those for the latter compound being consistent with the X-ray diffraction results [25]. This allows the authors to be confident of the analysis made for Tp*VO$(OMe)_2$ and V-BrPO. The V–OMe distance, as determined by EXAFS, is shorter (1.77 Å) than the V–O-4-C_6H_4Br bond distance (1.848 Å from EXAFS and X-ray diffraction). It should be noted here that chloro(alkoxo) complexes have even shorter vanadium–alkoxo-oxygen bond lengths [25], as seen from Table 1. A valuable compilation of V=O and V–alkoxo-oxygen bond lengths as determined by X-ray crystallography is provided [8]. The V–alkoxo-oxygen bond lengths cluster around 1.78 Å. Analyses of EXAFS data suggest that the vanadium in V-BrPO could have a coordination number lower than six, and that the number of bound imidazole could be two at most. The authors suggest that the models investigated may not be appropriate for the overall structure [8].

In conclusion, and focusing particularly on the most recent results concerning the modeling of the vanadium site in V-BrPO, alkoxo ligands could in some ways account for the 1.72 Å distance observed in the EXAFS studies of the enzyme. Also the vanadium(V) in this case is more difficult to reduce, and this correlates with the high-energy LMCT. V-BrPO exhibits a LMCT transition as a shoulder near 315 nm [17]. When considering the reduced enzyme and η^1-carboxylatovanadium(IV) complexes, similar V–O bond lengths of 1.91 Å and 2.00 Å, respectively, have been observed, but there is no model carboxylato complex available in the Tp/Tp* vanadium(V) series [20]. However, there is no explanation of the large high-field shift in the ^{51}V NMR spectrum of about δ −1200 in V-BrPO. Similarly, EXAFS data on model compounds suggest that a five-coordinate structure might be present in the enzyme [8].

2.2.3. Carboxylato-bridged vanadium complexes

In Section 2.2.1., an η^1-benzoato-vanadium(IV) complex has been described. The same authors have also obtained a peculiar asymmetrical μ-malonato-complex from

Tp*VOCl(Me$_2$pzH) and sodium malonate. It is formulated as Tp*VO(μ-malonato)VO(Me$_2$PzH)Tp* (**13**) on the basis of an X-ray crystal structure determination [20]. The bridging dicarboxylate is monodentate to the Tp*VO(Me$_2$pzH) moiety, a bridging carboxylate between Tp*VO(Me$_2$pzH) and Tp*VO units and a six-membered chelating carboxylate to the Tp*VO unit. It is the first occurrence of such a coordination mode in an isolated dinuclear structure. This complex shows a 15-line pattern in its liquid-solution EPR spectrum with A_{iso} (50.5 G) being about half A_{iso} in mononuclear vanadium(IV) complexes (A_{iso} = 101.2 G for the η^1-benzoato complex). Weak antiferromagnetic coupling between the vanadium (about 3 cm^{-1}) is observed.

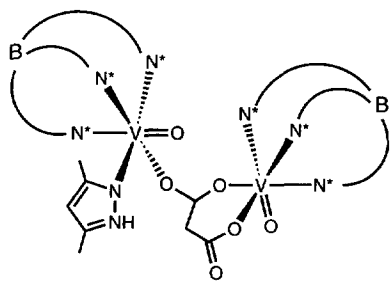

13

Two Tp(μ-oxo)(μ-carboxylato)V^{III} dinuclear species have also been isolated and the exchange coupling interactions have been studied. Green $Tp_2V_2(\mu\text{-}O)(\mu\text{-}CH_3CO_2)$ exhibits weak ferromagnetic exchange coupling with g = 2.2(1), J = +5(1) cm^{-1}. The value of μ_{eff} per V^{III} atom increases from 3.18 μ_B at 298 K to 3.36 μ_B at 98 K [28a]. Later, very strong ferromagnetic coupling was found in related triazacyclononane complexes [28b]. The μ-propionato-analog has also been fully characterized and found to exhibit similar ferromagnetic coupling (S = 2 ground state) with μ_{eff} = 3.46 μ_B per V^{III} atom. However, the μ-hydroxo cation afforded by protonation $[Tp_2V_2(\mu\text{-}OH)(\mu\text{-}CH_3CH_2CO_2)][CF_3SO_3]$ exhibits antiferromagnetic behavior with an S = 0 ground state (g = 2.01(1); J = −31.3(2) cm^{-1}) [29]. The X-ray crystal structures of both neutral μ-oxo (**14**) and cationic μ-hydroxo (**15**) complexes have been obtained. Upon protonation, the vanadium–bridging oxygen bond length increases from 1.777 Å to 1.933 Å. Unexpectedly, the V–O–V angle decreases from 133° to 123°. The authors suggest that there is a change in the hybridization of the oxygen bridge. Some sp character at the oxygen in the neutral dimer, caused by π-bonding with the oxophilic vanadiums and reinforced by the cobridging of the carboxylate, is lost upon protonation. From orbital considerations, the switchover from ferromagnetic to antiferromagnetic coupling is proposed to result from the decrease of the bridge angle, favoring increased antiferromagnetic coupling, and from the increase of the V–O bond lengths favoring decreased ferromagnetic coupling [29]. Mention of related studies involving substituted triazacyclononanes, which

can be considered as neutral analogs of Tp and Tp* ligands, should be made here [28,30,31].

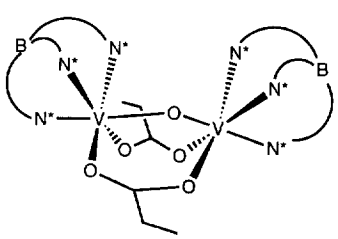

14

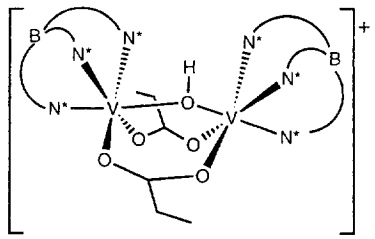

15

3. Niobium and tantalum

The early attempts to explore the chemistry of hydridotris(pyrazolyl)borato complexes of niobium and tantalum were hampered by several synthetic problems identified by the few groups then working in the area. These efforts were directed toward the synthesis of complexes with the metal in oxidation state IV or V. However, the more recent investigations into the area of niobium(III) alkyne complexes have been more successful. For these historical and chemical reasons, the chemistry of the oxidation states IV and V is presented first, the oxidation state III being dealt with later. As far as we are aware, no data have ever been published on other oxidation states for these two metals. We are excluding from the discussion the somewhat related bis(pyrazolyl)borato [32,33] and tris(pyrazolyl)methane complexes [34].

3.1. Niobium and tantalum(IV) and (V)

The first complex described with the heavier Group 5 metals $TpNbO(OMe)_2$ was unexpectedly obtained from $[NbCl_2(OMe)_3]_2$ and KTp in 41% yield. Ether elimination is proposed to occur. A $\nu(Nb{=}O)$ at 920 cm^{-1} was observed. However, the ^1H NMR spectrum between −45 and +60 °C revealed only one type of pyrazole ring, which argues against the proposed tridentate facial coordination of Tp [35]. This facial coordination leads to a 1:2 intensity pattern for the pyrazolyl protons as observed for Tp^*MOCl_2 (M is Nb or Ta) (see below).

Later reports showed that direct reactions of the pentahalides with either KTp or KTp* give complex mixtures of products involving either reduction or side-reactions such as B–N bond cleavage. In the case of $NbCl_5$ and KTp, the importance of the solvent and reaction temperature for the success of the syntheses is stressed [36]. The use of toluene or THF leads to unidentified oxo species, whereas dichloromethane and acetonitrile, either singly or as mixtures, give better results. Remarkably, only ionic niobium(V) species are obtained from the reaction mixtures. Thus,

$K[TpNbCl_5]$ is obtained in 58% yield according to Eq.(5). This salt precipitates during the course of the reaction, and the niobium(IV) dimer $Tp_2Nb_2Cl_6$ remains in solution.

$$NbCl_5 + KTp \xrightarrow{MeCN, -30\,^{\circ}C} K[TpNbCl_5] + Tp_2Nb_2Cl_6 \quad (5)$$

The niobium(IV) dimer can be obtained in better yield (72%) from $NbCl_5$ and KTp in dichloromethane/acetonitrile mixtures under reflux, or from $NbCl_4$ and KTp in acetonitrile. If $NbCl_4(MeCN)_3$ is used in the reaction with KTp, the ionic product $K[TpNbCl_4]$ is formed in 75% yield. The niobium(IV) dimer $Tp_2Nb_2Cl_6$ can be oxidized *in situ* with CCl_4, precipitating $TpNbCl_4$ (**16**) in 88% yield as dark red crystals. Despite this seemingly straightforward access to what should be a very attractive starting material, no further work on this compound has ever been reported.

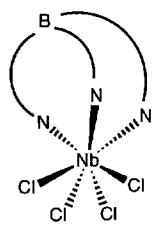

16

The ^1H NMR spectrum of $TpNbCl_4$ implies equivalent pyrazolyl groups, with doublets at δ 8.27 and δ 8.12 for the 3- and 5-protons, respectively, and a triplet at δ 6.81 assigned to the 4-proton. This spectrum suggests the heptacoordinate niobium. The need for highly pure CD_3CN solvent for the NMR analyses is emphasized. Traces of water induce B–N bond cleavage, as evidenced by a characteristic pyrazole NH signal.

When two equivalents of KTp are used, only dimeric niobium(IV) complexes are formed. Starting from $NbCl_5$ in MeCN at $-30\,^{\circ}C$, $Tp_2Nb_2Cl_6(pzH)_2$ is isolated in 30% yield, demonstrating the ready B–N bond cleavage. From $NbCl_4$ under refluxing conditions, $Tp_4Nb_2Cl_4$ is formed. This species is also available from three equivalents of KTp and $NbCl_5$ under similar conditions [36]. The niobium(IV) complexes are formulated as dinuclear on the basis of the observed diamagnetism and the well-resolved ^1H NMR spectra. Vapor-pressure osmometry and mass spectrometry data are also consistent with a dimeric formulation. These dinuclear species all exhibit a 1:2 intensity pattern for the pyrazolyl protons in their ^1H NMR spectra, and structures involving Cl bridges and bidentate Tp coordination have been proposed. Related bis(pyrazolyl)boratoniobium complexes have been also described [36].

Although very few details are provided, Tp^*NbCl_4 is one of the products (41%) of the reaction between $NbCl_5$ and KTp* in dichloromethane [37]. The salt $[HB(Me_2pz)_3BH][NbCl_6]$ is also obtained in 31% yield, the tantalum analog being

crystallographically characterized. Obviously, B–N bond cleavage reactions are occurring again and, as observed with Tp [36], the course of the reactions is solvent-dependent. The trispyrazolyl complex $Tp^*NbCl(Me_2pz)_3$ has been characterized by ^1H NMR spectroscopy [37]. No full paper has appeared.

The reaction of $TaCl_5$ with different pyrazolylborate salts gives mixtures of products [36–38]. However, alkyltantalum(V) complexes have been obtained according to Eq. (6).

$$TaMe_3Cl_2 + KRBpz'_3 \rightarrow RBPz'_3TaMe_3Cl + KCl \quad (6)$$

where $RBpz'_3$ is Tp, Tp*, pzTp.

Slow addition of the pyrazolylborate salt to $TaMe_3Cl_2$ in dichloromethane (KTp*) or diethylether (KTp, KpzTp) at low temperature gives $RBpz'_3TaMe_3Cl$ in respectable yield (52–66%). These complexes are much less reactive than $TaMe_3Cl_2$, which burns in air, and also more stable than $CpTaMe_3Cl$, which decomposes over a period of days. They are stable for months under dinitrogen and may be handled briefly in air [38].

Tp^*TaMe_3Cl is even less reactive. No chloride replacement with LiMe, MeMgCl, $PhCH_2MgCl$, KO-*t*-Bu or NaOMe has been noted. No reaction takes place with added MeOH, *t*-BuOH or *t*-$BuNH_2$. Even CO and CN-*t*-Bu are inert [38].

The X-ray crystal structure of $TpTaMe_3Cl$ confirms the seven-coordination. The geometry is that of a capped octahedron with a methyl group in the capping position as shown (**17A**). The tantalum–carbon bonds vary between 2.20(1) and 2.25(1) Å. Although there is no axis of symmetry, there are only minor deviations from an idealized geometry.

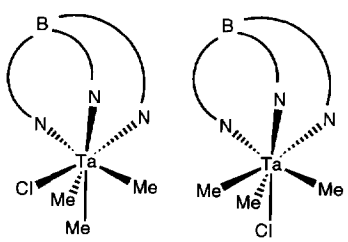

17A **17B**

The same structure is adopted by Tp^*TaMe_3Cl in solution. ^1H and ^{13}C NMR spectrocopies reveal a 1:2 intensity pattern for the Tp* and Ta–Me resonances, implying a plane of symmetry. The ^1H NMR Ta–Me signals appear at δ 2.50 (3H) and 1.31 (6H), and ^{13}C NMR Ta–Me signals at δ 101.2 and 87.9 appear as quartets with $^1J_{CH} = 121$ Hz. However, $TpTaMe_3Cl$ and $pzTpTaMe_3Cl$ exist as a mixture of two structures, one with a methyl group in the capping position as in the crystal structure (structure **17A**) and the other one with the chloro in the capping position (structure **17B**).

In structure **17B**, each set of Tp protons gives rise to only one signal in the ^1H NMR spectrum, whereas in structure A a 1:2 intensity pattern is observed. The two isomers are present at −8 °C. When the temperature is raised, the first, lower-energy process exchanges the Ta–Me resonances in isomer **17A**, leaving the pyrazolyl signals unchanged. A second higher-energy process scrambles all the Ta–Me signals of the two isomers. The low-energy process is proposed to be the rotation of the triangular face formed by three methyl groups, whereas the higher-energy process would include the Cl in a similar mechanism. However pairwise exchange of one of the three facial ligands with the ligand in the capping position was not excluded. There is no exchange between coordinated and uncoordinated pyrazole rings in (pzTp)$TaMe_3Cl$ [38].

No other reports of chemistry with Nb or Ta in the oxidation state V appeared during the following ten years, presumably owing to the lack of easily accessible starting material and to the high kinetic stability of the rare alkyltantalum complexes known.

More recently, a new entry into the chemistry of this oxidation state has appeared. A controlled synthesis of Tp* oxo and *tert*-butylimido complexes is reported [10]. Here again, the choice of the solvent is crucial for the success of the syntheses. The reaction between $[NbOCl_3]_x$ and KTp* in MeCN affords Tp^*NbOCl_2 in 72% yield, whereas a similar reaction starting from $[TaOCl_3]_x$ in DMF yields Tp^*TaOCl_2 in 68% yield. These complexes are characterized as monomers on the basis of the observation of a molecular ion in the mass spectra (**18**).

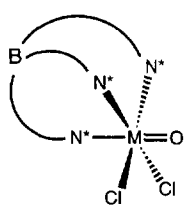

18 M = Nb, Ta

The 1:2 intensity pattern in the ^1H NMR spectra imply a symmetry plane in these complexes. In the IR spectra, ν(Nb=O) and ν(Ta=O) are observed at 936 and 932 cm^{-1}, respectively [10]. The analogous Cp or Cp* derivatives are unknown for niobium (only clusters are known: see, for example, Ref. [39]), and $[Cp^*TaOCl_2]_2$ is a dimer, unstable in solution [40]. The sulfidoniobium analog, Tp^*NbSCl_2, is also mentioned in a footnote [10], but the assignment of an IR band at 852 cm^{-1} to a ν(Nb=S) is questionable. A reported strong absorption at 516 cm^{-1} might be a better assignment.

Reaction of MCl_3py_2(N-*t*-Bu) (M is Nb, Ta) with KTp* in MeCN affords the corresponding imido complexes Tp^*MCl_2(N-*t*-Bu) (**19**) in 92% (Nb) and 56% (Ta) yields [10]. Analytical and spectroscopic characterization includes a strong ν(Nb=N–C) band at 1231 cm^{-1} in the IR spectrum. The chemistry of imido complexes has been reviewed [41,42], and this assignment is consistent with current knowledge.

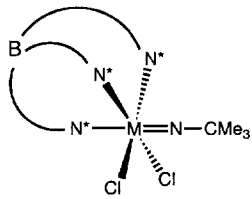

19 M = Nb, Ta

The difference $\Delta\delta$ between the ^{13}C NMR chemical shift of the quaternary carbon Cα bound to nitrogen and that of the methyl carbon Cβ of the *tert*-butyl imido group has been used to assess the amount of π-donation of the imido lone pair into an empty metal orbital [42,43]. The $\Delta\delta$ trend in the Group 5 Tp* imido complexes is V (56.1) > Nb (40.75) > Ta (34.6), with the vanadium complexes exhibiting a more electrophilic imido nitrogen [10]. The analogous Cp and Cp* complexes are known. For the Cp complexes the observed $\Delta\delta$ order is Nb (39.6) > Ta (34.3), and in the Cp* series Nb (38.4) > Ta (33.2) [44,45]. When comparing Cp, Cp* and Tp* complexes, either no obvious trend (Ta) or else small differences (Nb) are seen, and there is clearly no obvious interpretation.

No further chemistry appeared with these oxo and imido complexes until early 1995. We have ourselves unsuccessfully tried to make dialkyl, diaryl, dihydride and alkylidene oxo complexes starting from Tp^*NbOCl_2, but extensive decomposition reactions were observed in all cases [46]. Because of the more flexible stereoelectronic properties of the imido ligands, it is possible that more stable complexes might be obtained in the imido series.

3.2. Niobium(III)

A convenient entry into the formally Tp^*Nb^{III} chemistry with internal alkynes as coligands has been discovered, and some chemistry, either at the metal or at the alkyne, is being explored. In most of these complexes, the alkyne behaves as a four-electron donor, e.g. both π-systems are involved in the bonding to the metal. A detailed review on such alkyne behavior in Group 6 metal complexes has appeared [47], and basically all the conclusions are also valid for the Group 5 complexes. Structural comparisons have been made of the different behavior of alkynes within the Group 5 complexes [48].

The first subsection below is devoted to the dichloro(alkyne) complexes with either Tp or Tp* as coligand, with a special emphasis on comparison of structural data with that of analogous Cp or Cp* complexes. Alkyne elaboration reactions are included in this section since they directly correlate with geometrical features. The second section deals with hydrocarbyl complexes, and finally alkyne coupling reactions are described.

3.2.1. Dichloro(alkyne) complexes and alkyne alkylation reactions

Good yields (over 80%) of the red-purple $Tp^*NbCl_2(PhC{\equiv}R)$ can be obtained from the reaction of $NbCl_3(DME)(PhC{\equiv}CR)$ with KTp* in THF according to

Eq. (7). The original communication [49] describes the reaction of phenylpropyne (R is Me), but other derivatives have now been synthesized with other alkynes (R is Et, *n*-Pr or Ph, and 2-butyne) [50]. More recently, this reaction scheme has been applied to the synthesis of some unsubstituted Tp complexes $TpNbCl_2(RC{\equiv}CR')$, with $RC{\equiv}CR'$ being $PhC{\equiv}CMe$, $MeC{\equiv}CMe$, or $Me_3SiC{\equiv}CSiMe_3$ [51].

$$NbCl_3(DME)(PhC{\equiv}CR)+KTp' \xrightarrow{THF} Tp'NbCl_2(PhC{\equiv}CR)+KCl+DME \quad (7)$$

where Tp′ is Tp or Tp*

The X-ray crystal structures of both phenylpropyne complexes [49,51] show that the alkyne lies in the molecular mirror plane as shown (**20,21**), with an overall octahedral coordination around the niobium if the alkyne is considered to occupy one coordination site. As observed for some vanadium compounds, there are only minor structural differences between the two structures. In $Tp^*NbCl_2(PhC{\equiv}CMe)$, the niobium-coordinated alkyne carbon bond lengths are [49] 2.050(9) and 2.093(9) Å, averaging 2.07 Å, whereas in $TpNbCl_2(PhC{\equiv}CMe)$ these bonds lengths are 2.065(6) and 2.071(6) Å [51]. The Nb–C bonds are short and approach the range expected for niobium–carbon double bonds. They are typical of four-electron alkyne coordination [47], and compare well with those of analogous niobium and tantalum alkyne complexes [48]. The coordinated C–C bond length of the alkyne is 1.31(1) Å for the Tp* complex [49], and 1.301(8) Å for the Tp complex [51]. The four-electron donor alkyne exerts some *trans* influence, the Nb–N bond *trans* to it being at least 0.07 Å longer than the other two. Although the niobium in these complexes is formally d^2, Nb^{III} with 16 valence electrons, the alkyne appears to be substantially reduced, and metallacyclopropene tautomeric forms with a d^0, Nb^V configuration should be taken into account. For this reason and to make it clear that the alkyne is not a conventional two-electron donor, the metallacyclopropene form will be adopted in the drawings; see **20** and **21**.

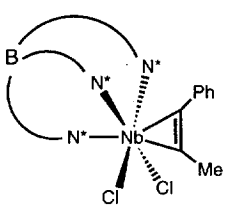

20

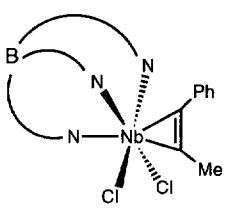

21

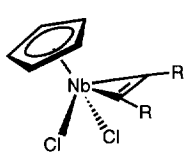

22

Isoelectronic Cp or Cp* niobium and tantalum complexes have been obtained previously in which the alkyne also behaves as a four-electron donor. The structural parameters for the metal–alkyne coordination do not differ significantly [52,53]. However, the overall geometry is different for the Cp and the Tp families. In the Cp (or Cp*) case, the alkyne is found to be parallel to the Cp plane as shown (**22**) (horizontal geometry). The only known exception is that of the Ta complex, which possesses a benzyne lying in the molecular plane [54]. In the Tp family, the whole phenylpropyne lies in the molecular mirror plane which bisects the Cl–Nb–Cl angle (vertical geometry). The phenyl ring always sits between two *cis*-pyrazole rings. The exact reason for these different ground-state geometries is not fully understood. The initial proposal in the Tp* case [49] favored steric interactions, even though the Tp complex is much less sterically hindered. Preliminary extended Hückel molecular orbital calculations on the model system $TpNbCl_2(HC{\equiv}CH)$ show that there is only a very small energy difference between the vertical and horizontal geometries, the former being more stable [55]. Similar calculations for horizontal $CpNbCl_2(HC{\equiv}CH)$ have also been carried out, and the barrier to acetylene rotation computed to be about 6 kcal mol^{-1} [53]. Vertical coordination of alkene and alkyne has been shown to result from orbital control in the d^6 iridium complex $TpIrH_2$(cyclooctene) [56], and in the d^4 tungsten complex $[Tp^*W(CO)_2(PhC{\equiv}CMe)]^+$ [57].

In both the Tp and Tp* series the vertical geometry is retained in solution. For the Tp* complexes containing non-symmetrical alkyne, two discrete isomers are observed by NMR spectroscopy at room temperature. The ratio of the two isomers depends on R, but the major isomer always has the phenyl group towards the *cis*-pyrazole rings. In the phenylpropyne case, no broadening of the ^1H NMR signals of the two isomers in toluene-d_8 is observed up to 373 K [49], whereas in the 2-butyne case, two alkyne methyl signals are observed at room temperature, and coalescence is reached at 358 K, giving a barrier to 2-butyne rotation of 16.3 kcal mol^{-1} [50]. In the Tp case, the phenylpropyne and 2-butyne show a single set of signals, whereas, for $TpNbCl_2(Me_3SiC{\equiv}CSiMe_3)$, coalescence of the methyl signals occurs at 273 K, leading to a barrier to alkyne rotation of 12.3 kcal mol^{-1} [51].

The deshielded coordinated alkyne carbon resonances in the ^{13}C NMR spectra of the complexes clearly prove that the alkyne also behaves as a four-electron donor in solution. The empirical criterion was first proposed by Templeton and Ward [58] and applied to other Group 6 metal complexes [47]. For $Tp^*NbCl_2(PhC{\equiv}CMe)$, the resonances are found at δ 264.5 and 218.7 (major isomer) or δ 247.6 and 232.6 (minor isomer) [49]. For the analogous Tp complex they are observed at δ 253.8 and 231.8 [51]. Values at higher field, with chemical shift values never higher than about δ 160, are found for two-electron alkyne ligands [59]. In the Cp family with either niobium or tantalum, similar ^{13}C chemical shifts are observed [52,53].

From the structural and spectroscopic data, there are obviously few differences between the Tp and Tp* ligands in these dichloro complexes with the exception of the height of the barrier to alkyne rotation. However, as observed with vanadium, there are notable differences in the electrochemical behavior. $Tp^*NbCl_2(PhC{\equiv}CMe)$ undergoes a reversible one-electron reduction at -1.19 V with a peak-to-peak

separation of 0.15 V and a peak intensity ratio of 0.9, whereas for the Tp complex these parameters are −0.93 V, 0.25 V and 0.5, respectively [50]. This is consistent with Tp* being more electron-rich than Tp, but also with the idea that Tp* imparts more kinetic stability than Tp, undoubtedly mainly for steric reasons.

That steric influence is a significant part of the unique ligating properties of these ligands also manifests itself in the only comparative reactivity study available to date. Indeed $Tp^*NbCl_2(PhC{\equiv}CMe)$ does not react with NaCp·DME, whereas a smooth reaction is observed in the case of $TpNbCl_2(PhC{\equiv}CMe)$, Eq. (8), giving yellow TpCpNbCl(PhC≡CMe) (**23**) in 75% yield [51].

$$TpNbCl_2(PhC{\equiv}CMe) + NaCp{\cdot}DME \longrightarrow TpCpNb(Cl)(PhC{\equiv}CMe) + NaCl + DME \quad (8)$$

This complex now has a d^2 configuration with 18 valence electrons for the niobium. The Cp ring is η^5-bound, a single ^1H NMR line being observed down to 193 K. The alkyne now behaves as a two-electron donor, as shown by the higher field shift of the coordinated carbon atoms (δ 163.5 and 152.9). Two discrete isomers in a 1:5 ratio are observed, with no indication of interconversion up to 373 K. The geometry of the complex is fully defined by an X-ray structure determination which shows that the alkyne, except for the phenyl ring, is now parallel to the Cp plane, as shown. It no longer bisects the two *cis*-pyrazole rings. In this geometry the alkyne eclipses one Nb–N(pyrazolyl) bond. The Cl, Nb and coordinated alkyne carbon atoms are nearly coplanar, so that the geometry is fully reminiscent of that observed in the bent metallocene series $Cp_2MX(RC{\equiv}CR')$ (M is Nb or Ta), a typical example of which is $(\eta^5\text{-}C_5H_4SiMe_3)_2NbCl(PhC{\equiv}CPh)$ [59]. The two-electron donor behavior of the phenylpropyne in TpCpNbCl(PhC≡CMe) is inferred from longer Nb–C bonds (2.146(3) and 2.165(3) Å) and a shorter C–C bond (1.254(4) Å) as compared to those in $TpNbCl_2(PhC{\equiv}CMe)$ [51]. Surprisingly here, either Cp or Tp can independently dictate the ground-state geometry in the 16-electron, Nb^{III} d^2 species containing a four-electron donor alkyne, whereas direct intramolecular competition between the two ligands leads to a Cp-driven ground-state geometry. In the absence of extended Hückel calculations, the reasons for this are still under debate [51].

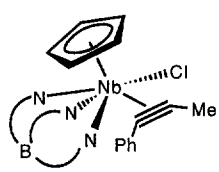

23

Attempts to functionalize the alkyne diastereoselectively, taking advantage of the vertical coordination in chiral Tp*Nb(Cl)(OMe)(PhC≡CR), have been made using deprotonation–alkylation sequences [60]. Propargylic protons of four-electron donor alkynes in Group 6 metal complexes are acidic [61–63], and

Tp*$NbCl_2$(PhC≡CMe) can be cleanly deprotonated with Li-*n*-Bu·TMEDA at low temperature. Subsequent addition of MeI or $PhCH_2Br$ gives good yields of the alkylated alkyne complexes Tp*$NbCl_2$(PhC≡CCH_2R) (R is Me, CH_2Ph), Eq. (9). Despite the known high reactivity of Nb–Cl bonds towards anionic nucleophiles, no side-products are formed. Other bases such as Li-*n*-Bu, Li-*t*-Bu and $LiN(SiMe_3)_2$ do not promote clean reactions [60].

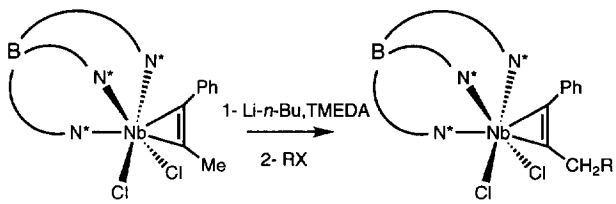

(9)

Similar results are obtained from the chiral complex Tp*Nb(Cl)(OMe)(PhC≡CMe), the characterization of which is described below. Starting from Tp*Nb(Cl)(OMe)(PhC≡CCH_2Me), addition of the base and then $PhCH_2Br$ gives Tp*Nb(Cl)(OMe)[PhC≡$CCHMe(CH_2Ph)$] in 90% yield as a 4:1 mixture of two diastereomers A and B. Starting from Tp*Nb(Cl)(OMe)[PhC≡CCH_2CH_2Ph] and adding MeI to the deprotonated complex gives the same complex Tp*Nb(Cl)-(OMe)[PhC≡$CCHMe(CH_2Ph)$] with a 1:6 diastereomeric ratio (A:B). Hence the chiral auxiliary Tp*Nb(Cl)(OMe) allows for some minimal diastereoselectivity in these alkyne alkylation reactions. This may be ascribed to the existence of alkyne rotational isomers and to a low facial discrimination due to the similar size of chloro and methoxo [60]. Similar diastereoselective reactions have been performed fully using the chiral auxiliary Tp*W(I)(CO) [64]. An X-ray diffraction study for Tp*Nb(Cl)(OMe)[PhC≡$CCHMe(CH_2Ph)$] (**24**) gave an unexpected result. The stereogenic propargylic carbon atom is trigonal planar, and the methyl group attached to it has a large thermal ellipsoid, the principal axis of which is perpendicular to the plane around the propargylic carbon. This disorder may be accounted for by the fact that both configurations of the propargylic carbon are present in the crystal for a given niobium configuration. The ^1H NMR spectrum on a solution of the single crystal used for the X-ray diffraction study showed both diastereomers in a ratio of about 1:3 [60].

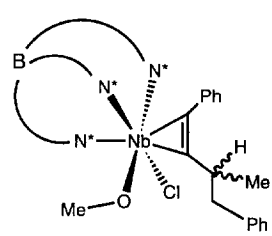

24

3.2.2. Hydrocarbyl derivatives

Both mono- and di-hydrocarbyl complexes have been synthesized, starting from the dichloro(alkyne) complexes or from the chloro(methoxo) derivatives which are the original starting materials.

The orange-yellow chloro(methoxo) complexes Tp*Nb(Cl)(OMe)(PhC≡CR) are obtained straightforwardly in high yield by reaction of Tp*$NbCl_2$(PhC≡CR) with sodium methoxide in THF [65]. These are chiral molecules with the niobium as the stereogenic center, as shown by a 1 : 1:1 intensity pattern for each type of Tp* proton and carbon atom. Although the alkyne still behaves as a four-electron donor, the resonances of the coordinated alkyne carbon atoms are shifted to higher field in the ^{13}C NMR spectra. This undoubtedly reflects the good π-donating ability of the methoxo, which reduces the alkyne contribution to the electron density at the metal. For example, the niobium-bound alkyne carbons resonate at δ 264.5 and δ 218.7 in Tp*$NbCl_2$(PhC≡CMe), but they are found at δ 219.3 and δ 189.6 in Tp*Nb(Cl)(OMe)(PhC≡CMe) [65].

Methyl-niobium and phenyl-niobium species (**25**) are formed readily in high yield from Tp*Nb(Cl)(OMe)(PhC≡CR) and the appropriate lithium reagent [65]. In the ^{13}C NMR spectrum the carbon attached to niobium gives rise to a broad quartet at δ 38.2 ($^1J_{CH}$ = 120 Hz) for Tp*Nb(Me)(OMe)(PhC≡CEt) and as a broad singlet at δ 198.1 for Tp*Nb(Ph)(OMe)(PhC≡CEt). The diastereotopic methylene alkyne protons in Tp*NbXY(PhC≡CEt) are inequivalent in the ^1H NMR spectrum in all complexes, whatever X and Y, except for Tp*Nb(Ph)(OMe)(PhC≡CEt), in which they appear as a single quartet. Although rotation around the niobium–phenyl bond can be frozen out, the single quartet is independent of solvent and temperature. There is no suitable explanation for this deceptively simple spectrum [65]. These hydrocarbyl species undergo some reactions, described in Section 3.2.3.

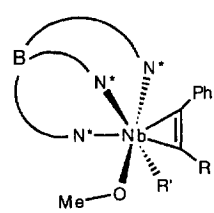

25, R' = Me, Ph

Longer-chain, linear alkyl groups also form stable complexes, although β-hydride elimination is common for that kind of alkyl. Furthermore, some of these complexes exhibit α-agostic interactions (3-center, 2-electron bond) virtually unknown when β-hydrogen atoms are present [66,67].

Ethyl and *n*-propyl complexes of the type Tp*Nb(Cl)(Et)(PhC≡CR) and Tp*Nb(Cl)(*n*-Pr)(PhC≡CR) (R is Me, Et, *n*-Pr, Ph) (**26**) are synthesized in 80% yield from dichloro precursors and the appropriate Grignard reagent in toluene [68,69]. The ^1H NMR data show that one proton of the niobium-bound methylene group is notably deshielded, while the other is shielded. In

Tp*Nb(Cl)(CH_2Me)(PhC≡CMe) these protons appear at δ 3.84 and δ 0.37 as doublets of quartets [68], while in Tp*Nb(Cl)(CH_2CH_2Me)(PhC≡CMe) they are found at δ 3.69 and δ 0.58 [69]. The large chemical shift difference is noteworthy, but evidence for the α-agostic interaction comes from the ^{13}C NMR spectra. Small $^1J_{CH}$ values indicate a weakened C–H bond, and this is one of the most reliable indications of agostic interactions in solution [66,67]. For Tp*Nb(Cl)(CH_2Me)(PhC≡CMe), the α-carbon atom produces a niobium-broadened doublet of doublets at δ 86.5 with $^1J_{CH}$ 108 and 129 Hz [68]. For Tp*Nb(Cl)(CH_2CH_2Me)(PhC≡CMe), the α-carbon atom resonates at δ 95.9 as a doublet of doublets with $^1J_{CH}$ of 106 and 125 Hz [69]. More recently, measurement of the $^1J_{CH}$ from the ^{13}C satellites in the ^1H NMR spectrum of Tp*Nb(Cl)(CH_2Me)(PhC≡CPh) indicated that the shielded proton is associated with the low $^1J_{CH}$ [70], consistent with an α-agostic interaction [66,67]. The α-agostic interaction appears to be static, the ^1H NMR data being temperature-independent between 213 and 323 K.

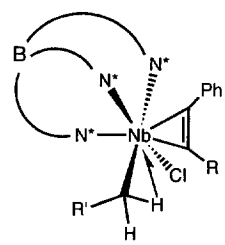

26, R′ = Me, Et

An X-ray crystal structure of Tp*Nb(Cl)(CH_2Me)(PhC≡CEt) also suggests that the α-agostic interaction is present in the solid state [68]. As a result of this three-center, two-electron bond, the Nb–Cα bond is shortened and the Nb–Cα–Cβ angle is opened. The Nb–Cα bond length is 2.17(2) Å and the Nb–Cα–Cβ angle is 126(1)°. These parameters can be compared to Nb–C single bonds of 2.316(8) and 2.31(1) Å, and to Nb–Cα–Cβ angles of 118.6(7) and 121(1)°, in $Cp_2Nb(CH_2Me)(C_2H_4)$ [71] and $Cp_2Nb(CH_2Me)$(MeC≡CMe) [72] respectively, in which no, or weak, agostic interactions are present. Other α-agostic alkyl Group 5 complexes have similar structural features. In CpNb(N-2,6-C_6H_3-*i*-Pr_2)(CH_2-*t*-Bu)$_2$, with two α-agostic interactions, the Nb–Cα bond lengths are 2.174(3) and 2.215(3) Å and the Nb–Cα–Cβ angles are 131.2(2) and 132.5(3)° [73]. Unfortunately, the accuracy of the structure of Tp*Nb(Cl)(CH_2Me)(PhC≡CEt) is not high, and hydrogen atoms have not been located. Also, no reduced ν(C–H) could be safely assigned in the IR spectra of these complexes [68].

The α-agostic interaction has been probed in other alkyl derivatives. The benzyl complex Tp*Nb(Cl)(CH_2Ph)(PhC≡CMe) is not agostic. It shows a small chemical-shift difference for the methylene protons of the benzyl group ($\Delta\delta$ = 0.74 ppm) and the α-carbon resonance is a triplet at δ 89.6 with a normal $^1J_{CH}$ of 120 Hz. The ethyl(methoxo) complex Tp*Nb(OMe)(CH_2Me)(PhC≡CMe) does not present a

clear-cut situation. The triplet feature ($^1J_{CH}=116$ Hz) of the α-carbon atom observed at room temperature vanishes at 183 K, suggesting a dynamic process averaging one large and one small $^1J_{CH}$. Any α-agostic interaction here is much weaker than in the chloro(ethyl) complexes [68]. The reasons for this are probably electronic, although the benzyl case may also be the result of some steric contribution. Methoxo is a better π-donor than chloro, and therefore competes more efficiently with a Cα–H bond for the available niobium orbital. Similarly the phenyl group may lower electron density at Cα. Other substitutions at Cα have been attempted, but only rearrangement products have been observed so far (see Section 3.2.3).

However, the important point is that an α-agostic interaction is preferred over a more common β-agostic interaction. Undoubtedly, this is due to the bulky Tp*, since β-agostic interactions require considerable space to bend the Cα round, whereas only a small distortion of the ethyl group is needed for the α-agostic interaction to occur [66,67]. A similar preference for α-agostic interaction is observed in $[Cp^*Hf(CH_2CHMe_2)(PMe_3)]^+$, which is obviously a crowded molecule [74]. β-elimination itself is usually more facile than α-abstraction in Group 5 metal complexes [75], although competition between the two processes has been observed [76]. Although Cp or Cp* Nb or Ta alkyne complexes are known, only methyls have been described in the hydrocarbyl series [54,77,78], so that no direct comparison can be made between Tp* and Cp or Cp* ligands. However, given the similarity in bonding interactions between alkyne and imido (for recent examples and references, see Refs. [79,80]), the β-hydride elimination, leading to $CpNb(N\text{-}2,6\text{-}C_6H_3\text{-}i\text{-}Pr_2)(PMe_3)(C_2H_4)$ from $CpNb(N\text{-}2,6\text{-}C_6H_3\text{-}i\text{-}Pr_2)Cl_2$, ethyl Grignard and PMe_3, is noteworthy [81].

Chloro(methyl) complexes Tp*Nb(Cl)(Me)(PhC≡CR) from the rearrangement of α-agostic phenylpropyne complexes (see below) have been characterized, but their direct synthesis from $Tp^*NbCl_2(PhC{\equiv}CR)$ and the methyl Grignard is a tedious procedure, the compound being contaminated by remaining dichloro and dimethyl complexes. Only one pure complex has been obtained in this way [69]. However, $Cp^*Ta(Cl)(Me)(PhC{\equiv}CPh)$ is formed when $Cp^*TaMe_2(PhC{\equiv}CPh)$ is treated with isopropyl chloride in the presence of a catalytic amount of $AlCl_3$ [78].

The α-agostic species $Tp^*Nb(Cl)(CH_2R)(PhC{\equiv}CR')$ (R is Me or Et) undergoes a thermally induced rearrangement which exchanges the α-agostic alkyl group bound to the niobium with the alkyl group of the alkyne [69]. When R′ is Me, the reaction goes to completion and the methyl(niobium) derivatives $Tp^*Nb(Cl)(Me)(PhC{\equiv}CCH_2R)$ are formed [Eq. (10)]. Some $Tp^*NbCl_2(PhC{\equiv}CCH_2R)$ is also formed, but no $Tp^*NbCl_2(PhC{\equiv}CMe)$. The rearrangement follows a clean first-order kinetic rate law with activation parameters (R is Me) $\Delta H^{\dagger}=113\pm5$ kJ mol^{-1} and $\Delta S^{\dagger}=4\pm12$ J K^{-1} mol^{-1}. There is no dependence upon the migrating *n*-alkyl group since the rate constants for ethyl and propyl groups are equal, $k(343K)=3.0\times10^{-5}$ s^{-1}. When the two migrating alkyl groups are able to form α-agostic bonds, an equilibrium is reached. Heating pure $Tp^*Nb(Cl)(Et)(PhC{\equiv}C\text{-}n\text{-}Pr)$ in toluene gives a roughly 1:1 mixture of $Tp^*Nb(Cl)(Et)(PhC{\equiv}C\text{-}n\text{-}Pr)$ and $Tp^*Nb(Cl)(n\text{-}Pr)(PhC{\equiv}CEt)$ [Eq. (11)]. A control experiment starting from $Tp^*Nb(Cl)(n\text{-}Pr)(PhC{\equiv}CEt)$ yields the same result.

Here intramolecular C–C bond activation is realized. Overall the reaction is a metathesis of niobium–carbon and carbon–carbon bonds. That the α-agostic bond is needed for these rearrangements to occur is further supported by the fact the η^1-benzyl complex merely decomposes under similar conditions. A mechanism based on alkyl migration to alkyne giving an η^2-vinyl intermediate has been proposed.

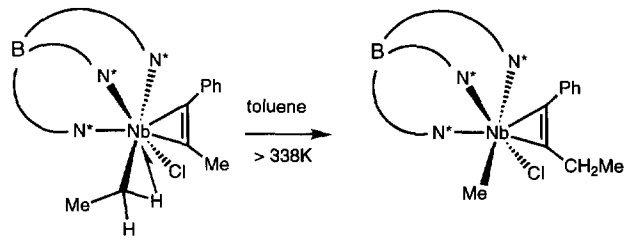

(10)

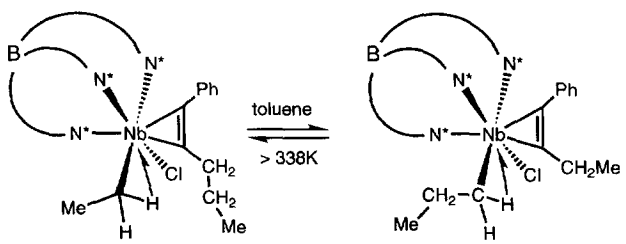

(11)

Some unpublished results from trapping experiments confirm that alkyl migration indeed occurs, but η^1-vinyl not η^2-vinyl complexes are isolated. Heating a mixture of Tp*Nb(Cl)(Et)(PhC≡CEt) and PhC≡CMe yields Tp*Nb(Cl)(η^1-CPh=CEt_2)(PhC≡CMe) [Eq. (12)], in which the entering phenylpropyne behaves as a four-electron donor (^{13}C NMR, δ 249.7 and 224.1) and the vinyl group is η^1-bound to the metal (Cα, δ 204.9) [82]. The η^2-vinyl coordination with a two-electron donor alkyne is not observed.

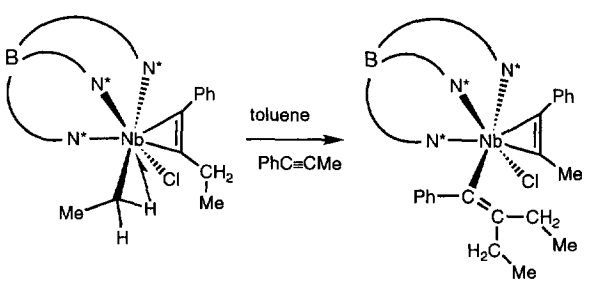

(12)

Other trapping experiments also show that a reactive intermediate is generated [Eq. (13)]. Propylene oxide and ethylene sulfide are deoxygenated or desulfurized, giving the heteroatom-bound niobium(V) species Tp*Nb(O)(Cl)(η^1-CPh=CEt_2) (ν(Nb=O)=930 cm^{-1}) and Tp*Nb(S)(Cl)(η^1-CPh=CEt_2) (ν(Nb=S)=514 cm^{-1}), respectively [82].

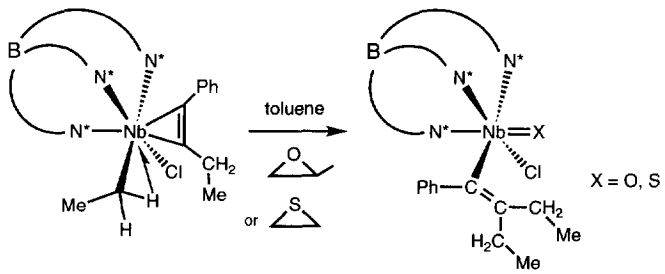

(13)

These rearrangements are noteworthy for several reasons. First, alkyl migration to a four-electron donor alkyne in Group 6 metal complexes is unknown, although η^2-vinyl complexes are formed from nucleophilic attack at an alkyne carbon atom [47]. Similarly, Tp*$NbMe_2$(PhC≡CR) [49] and the isoelectronic Cp complexes [77] are thermally stable. The reactions reported here are also rare examples of alkyne insertion into a transition metal–alkyl bond, the first step of alkyne polymerization via a vinyl pathway. Furthermore, α-agostic assistance has been demonstrated and the near-zero $\Delta S^{\dagger}$ value implies a transition state closely resembling the α-agostic complex. It has been suggested that α-agostic interactions assist alkyl migration to a bound olefin in Ziegler–Natta type polymerizations [67,83].

Finally, dimethyl derivatives are known [49]. Thermally stable dimethyl complexes are formed in high yield from Tp*$NbCl_2$(PhC≡CR) and two equivalents of methyllithium. A similar reaction of Tp*$NbCl_2$(PhC≡CMe) with two equivalents of benzyl Grignard yields the dibenzyl complex Tp*$Nb(CH_2Ph)_2$(PhC≡CMe) [84]. As already mentioned, analogous Cp/Cp* niobium and tantalum dimethyl complexes are known [77]. The reaction of two equivalents of ethyl Grignard with Tp*$NbCl_2$(PhC≡CMe) does not lead to a diethyl species but to a metallacyclic complex. This is described in the following section.

3.2.3. Alkyne coupling reactions

Different types of reaction which all lead to similar alkyne-coupled products, *e.g.* five-membered niobacycles, are described in this section.

The first is observed when excess carbon monoxide reacts with Tp*Nb(Me)(OMe)(PhC≡CR) or Tp*Nb(Ph)(OMe)(PhC≡CEt) [65]. The resulting five-membered oxaniobacycles Tp*(MeO)Nb[C(Ph)C(R)C(Me)O] (**27**) and Tp*(MeO)Nb[C(Ph)C(Et)C(Ph)O] are probably formed *via* undetected acyl (either η^1 or η^2) alkyne complexes. Similar reactions have been observed in the Cp series. The reaction of *t*-BuNC with $CpTaMe_2$(PhC≡CPh) leads first to the iminoacyl alkyne complex CpTa(Me)(η^2-MeCN-*t*-Bu)(PhC≡CPh), which subsequently rearranges to the azatantalacycle Cp(Me)Ta[C(Ph)C(Ph)C(Me)N-*t*-Bu] [77]. The same reaction with substoichiometric amounts of CO gives tractable products only in the Cp* case, and Cp*(Me)Ta[C(Ph)C(Ph)C(Me)O] is isolated [78]. No η^2-acyl complex could be detected. These comparisons show simply how Tp* allows the isolation of complexes not formed or less stable in the Cp series.

The second reaction type, which leads to a five-membered niobacycle containing

four carbon atoms, was observed during a study of the effects of substitution at Cα in the α-agostic complexes Tp*Nb(Cl)(CH_2R)(PhC≡CR′) (see section 3.2.2). The reaction of allylmagnesium chloride with Tp*$NbCl_2$(PhC≡CR′) does not yield an allyl product, and the alkyne-coupled products Tp*(Cl)Nb[C(Ph)C(R′)CHCHMe] (**28**) are formed in moderate yield. Presumably an η^1-allyl complex is formed first, and it couples with the alkyne and undergoes a 1,3-hydrogen shift, allowing ring closure [85]. Rearrangement of the allyl group to a prop-1-enyl prior to alkyne coupling is unlikely, since stable η^1-vinyl alkyne complexes have been isolated (see Section 3.2.2).

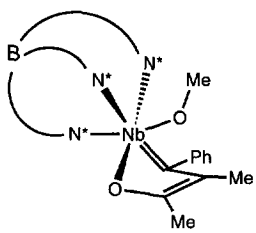

27

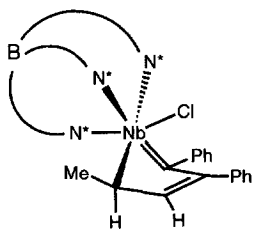

28

The last example of five-membered-ring formation was observed when two equivalents of ethylmagnesium chloride were added to Tp*$NbCl_2$(PhC≡CMe). The first equivalent gives the α-agostic ethyl complex Tp*Nb(Cl)(Et)(PhC≡CMe) rapidly, while the second equivalent reacts slowly over days, giving the formally dehydrogenated complex Tp*(Et)Nb[C(Ph)C(Me)$CHCH_2$] (**29**) [84]. There is no mechanistic information on this reaction. Apart from the five-membered ring, which is described below with the other compounds of this family, the ethyl group attached to the niobium certainly is α-agostic, with one of the diastereotopic methylene protons being highly shielded at δ −3.40, the other being at δ 1.80 in the ^{1}H NMR spectrum. They appear as doublets of quartets with J_{HH} = 6.6, 7.6 and 13.3 Hz. The doublet of doublets of the methyl group is observed at δ 0.73. The α-carbon bound to the niobium nucleus gives a broad doublet of doublets at δ 78.2 with $^1J_{CH}$ = 107 and 120 Hz in the ^{13}C NMR spectrum. The $^1J_{CH}$ from the ^{13}C satellites in the ^{1}H NMR spectrum indicate that the shielded proton is associated with the small $^1J_{CH}$, proving the α-agostic interaction [66,67,84].

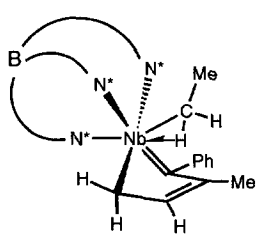

29

All these five-membered rings have similar ^{1}H and ^{13}C NMR properties. In addition, X-ray crystal structures have been obtained for Tp*(OMe)Nb[C(Ph)C(Me)C(Me)O] [65] and Tp*(Cl)Nb[C(Ph)C(Ph)CHCHMe] [85], and both compounds exhibit the same basic structure. The spectroscopic and solid-state data are fully consistent with the three resonance structures shown (**30**). They are characteristic of a general class of unsaturated carbene ligand η^n-C_nR_n+1, particularly well known in Group 6 metal complexes [86–88]. These data are similar to those of the isoelectronic aza- and oxa-tantalacycles Cp(Me)Ta[C(Ph)C(Ph)C(Me)N-*t*-Bu] [77] and Cp*(Me)Ta[C(Ph)C(Ph)C(Me)O] [78], which have been described as metallacyclopentatrienes (**31**) like other, more symmetrical Group 6 and Group 5 complexes such as Cp(Cl)Mo(C_4Ph_4) [77,89], $W(OR)_2(C_4Et_4)$ [90], and $Cp(PMe_3)V$[C(Ph)C(Ph)C(Me)C(Me)] [91]. It has been proposed that the oxa- and aza-metallacycles are forms intermediate between the two descriptions [85]. The same structures are obtained in the Tp* series from seemingly quite different rearrangements, so that formation of the folded five-membered rings can be considered as a driving force for the reactions or, alternatively, this type of metallacycle can be considered to be a potential well.

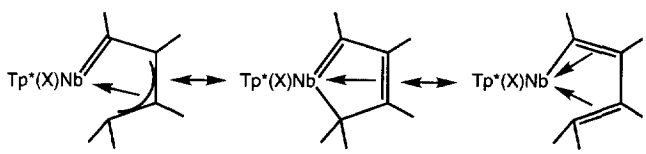

30

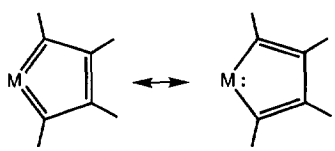

31

4. Recent work and conclusions

While this review was being written, new aspects of vanadium chemistry were described, and some recent results from the Laboratoire de Chimie de Coordination on the chemistry of niobium(I) are worth mentioning.

Reaction of either TpVO(acac) or Tp*VO(acac) with $P(OH)_2(OPh)_2$ in dichloromethane gives the dimers $[TpVO(\mu\text{-}PO_2(OPh)_2)]_2$ (**32**) or $[Tp^*VO(\mu\text{-}PO_2(OPh)_2)]_2$ (**33**) in 79% yield. There is little difference in the bonding parameters around the vanadium atoms between the Tp or the bulkier Tp* complexes. However, the distance between the two vanadium atoms in the dimers increases from 4.931(1) Å in **32** to 5.367(4) Å in **33**. This difference results principally from a flattening of the eight-membered ring constituting the bridge core, as shown. An almost ideal chair

conformation is adopted with Tp, whereas the core is close to planar with Tp*. $[TpVO(\mu\text{-}PO_2(OPh)_2)]_2$ exhibits weak ferromagnetic intradimer coupling. The EPR data at room temperature consist of a 15-line spectrum in low-to-moderate polarity solvents ($g = 1.962$, $A = 56$ G), typical of an exchange-coupled divanadyl complex. Transitions within the triplet are observed at 77 K. However, in DMF at room temperature an eight-line pattern is observed, indicating dissociation of the dimer. This spectrum is similar to that of $[Tp^*VO(\mu\text{-}PO_2(OPh)_2)]_2$, whatever the solvent ($g = 1.982$, $A = 100$ G). At 77 K, an anisotropic eight-line spectrum is observed, with no zero-field splitting effect ($g_{\parallel} = 1.947$, $A = 178$ G; $g_{\perp} = 1.986$, $A_{\perp} = 62$ G). The weak ferromagnetic coupling in **32** is a direct consequence of the geometry of the complex. Because of the location of the vanadyl oxygen atom with respect to the second vanadium, the ready delocalisation of the unpaired electron is achieved. Orthogonality between the V=O π-orbital and its own magnetic orbital leads to the ferromagnetic coupling. In the flattened structure of **33**, the interaction of a vanadyl unit with the neighboring vanadium decreases. Moreover, the increased V–V distance induces only a weak direct exchange. Both these phenomena lead to the observed uncoupled EPR spectrum [92].

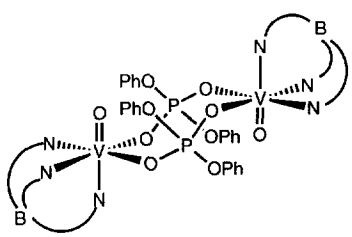

32

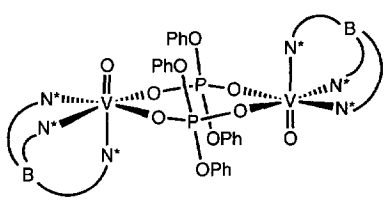

33

A unified classification of the conformations available for cyclic $(O)V(\mu\text{-}OPO)_2V(O)$ bridging units in phosphatovanadyl systems is provided. A clear correlation between geometric distortions and magnetic properties is drawn. The rationale behind this scheme seems to be general, and examples with sulfate and carboxylate that fit the classification are described [92].

In an earlier study [93], the attempted synthesis of the vanadium(III) analog of **32** starting from $Tp_2V_2(\mu\text{-}O)(\mu\text{-}CH_3CO_2)_2$ and excess diphenyl phosphate was shown to yield the trimetallic complex $\{TpV[\mu\text{-}PO_2(OPh)_2]_3\}_2Mg$ (**34**). The magnesium(II) ion comes from magnesium sulfate used as drying agent. In the crystal, a linear centrosymmetric structure is observed. The Mg^{II} ion is octahedrally coordinated to six bridging diphenylphosphates. Each $TpV[\mu\text{-}PO_2(OPh)_2]_3^-$ anion acts as a tridentate chelate. Starting from the vanadium(III) monomer $TpVCl_2(DMF)$ and sodium monophenyl phosphate, a tetrameric complex $\{TpV[\mu\text{-}PO_3(OPh)]\}_4$ (**35**) is obtained. The resulting cubane-like structure is formed owing to the tridentate monophenyl phosphate which bridges three TpV^{III} units. Thus there is a clear correlation between open metal-coordination sites and bridging ligand denticity. This allows a high degree of cluster size control. Comparison with the vanadium(IV)

cases is noteworthy. These studies illustrate new aspects of Tp chemistry, namely in the study of solid-state materials [93].

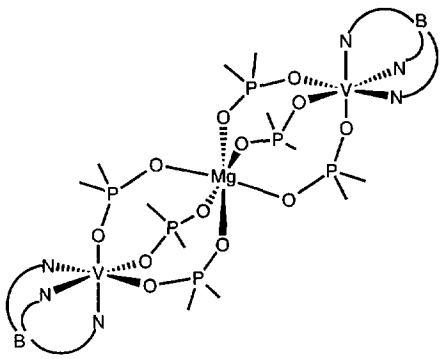

34

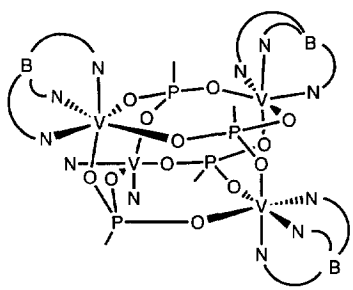

35

The 16-electron complex $Tp^*NbCl_2(PhC{\equiv}CMe)$ is conveniently reduced by an excess of sodium amalgalm under CO, yielding the niobium(I) dicarbonyl complex $Tp^*Nb(CO)_2(PhC{\equiv}CMe)$ [94]. Alkyne carbon atom resonances are observed at δ 259.4 and 212.2 in the ^{13}C NMR spectrum, consistent with a four-electron donor description for this ligand. The d^4 niobium(I) achieves an 18-valence electron count. The analogous 2-butyne complex gives a single ^1H NMR signal for both methyl groups, which splits into two below 208 K ($\Delta G^{\dagger} = 9.6$ kcal mol^{-1}), demonstrating again that the alkyne sits in the molecular mirror plane (**36**). This situation is akin to that found for the isoelectronic $[Tp^*W(CO)_2(PhC{\equiv}CMe)]^+$ [57] and orthogonal to that observed for $CpNb(CO)_2(PhC{\equiv}CPh)$ [95]. One CO in $Tp^*Nb(CO)_2(PhC{\equiv}CMe)$ is readily displaced by added phenylpropyne under refluxing conditions giving the bis(alkyne) complex, $Tp^*Nb(CO)(PhC{\equiv}CMe)_2$ (**37**) [94]. Coordinated alkyne carbon atom resonances are observed at δ 172.1 and 165.6, at much higher field than for $Tp^*Nb(CO)_2(PhC{\equiv}CMe)$. A plane of symmetry is evident from the ^1H NMR spectrum in the temperature range 178 to 373 K, and the X-ray crystal structure reveals the geometry shown below (**37**). Both alkynes are

parallel to the Nb–CO axis, with the methyl groups directed towards the CO. The Nb–alkyne carbon atom bond lengths are 2.133(3), 2.188(3), 2.140(3) and 2.185(3) Å, and the coordinated alkyne C–C bond lengths are 1.272(4) and 1.276(4) Å. These observations, and the high-field shift of the alkyne carbon atoms, indicate that the two alkynes now formally contribute six electrons to the total electron count, each alkyne behaving as a three-electron donor [47]. The observed geometry is similar to that previously observed for $CpNb(CO)(PhC{\equiv}CPh)_2$ [96]. Presumably the $d\pi$ splitting is dominated by CO in both structures.

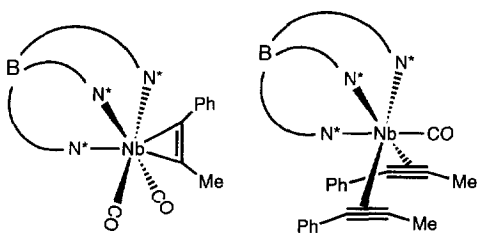

36 **37**

These recent examples, from inorganic vanadium chemistry and from organometallic niobium chemistry, show the dramatic and current utilization of the hydridotris(pyrazolyl)borates in the chemistry of the Group 5 transition metals. They also summarize some of the important features of the ligating properties of the hydridotris(pyrazolyl)borates. Comparison between Tp and Tp* indicates that steric variations lead to subtle changes outside the first coordination spheres, changes that may have important consequences for the physicochemical properties of the complexes. From a kinetic point of view, Tp* leads to stabilized species that are often transient in the case of Tp. Similarly, Tp and Tp* clearly allow for unique structures and reactivities when compared to the family of cyclopentadienyl ligands. However, the relatively easy B–N bond cleavage which sometimes occurs when the metals are in higher oxidation states has to be kept in mind. Nevertheless, considering the advances described in this review, further developments in the chemistry of the Group 5 transition metals (such as the organovanadium chemistry) with hydridotris(pyrazolyl)borato ligands are to be expected.

Note added during revision. During the time this article was being reviewed, the syntheses and crystal structures of $TpV(N\text{-}^tBu)Cl_2$ and $Tp^*V(N\text{-}2,6\text{-}i\text{-}Pr_2\text{-}C_6H_3)Cl_2$ have been reported. In the latter complex, the aryl ring sits in the molecular mirror plane, both in the crystal and in solution. In the presence of methylalumoxane, $Tp^*V(N\text{-}2,6\text{-}^iPr_2\text{-}C_6H_3)Cl_2$ catalyzes the polymerization of ethylene (14 kg mol^{-1} h^{-1}, Mw = 47000 and Mw/Mn = 3.0) and propylene (1 kg mol^{-1} h^{-1}, atactic polymer, Mw = 3800 and Mw/Mn = 2.0). Several alkoxo derivatives are also prepared [97] (see also Section 2.1.3).

Acknowledgements

I am indebted to Professor J.L. Templeton (University of North Carolina at Chapel Hill, USA), with whom the niobium chemistry started, for his steady interest in the subject. I also acknowledge Professor G.J. Leigh (University of Sussex, UK) and Dr P.W. Dyer for improving the English of the manuscript. I warmly thank the few first-year students who have contributed to some of the niobium chemistry (F. Biasotto, P. Lorente and P. Zeline). I thank Dr. R. Mathieu (LCC-CNRS, Toulouse) for giving me the opportunity to carry out the research which has been described in this review.

References

[1] (a) S. Trofimenko, Prog. Inorg. Chem., 34 (1986) 115–210; (b) S. Trofimenko, Chem. Rev., 93 (1993) 943–980.
[2] (a) K. Niedenzu and S. Trofimenko, Top. Curr. Chem., 131 (1986) 1–37; (b) P.K. Byers, A.J. Canty and R.T. Honeyman, Adv. Organomet. Chem., 34 (1992) 1–65; (c) G. Parkin, Adv. Inorg. Chem. (1995); (d) N. Kitajima and W.B. Tolman, Prog. Inorg. Chem. (1995); (e) D.L. Reger, Coord. Chem. Rev., in press; (f) I. Santos and N. Marques, New J. Chem., 19 (1995) 551–571.
[3] L.E. Manzer, J. Organomet. Chem., 102 (1975) 167–174.
[4] P. Dapporto, F. Mani and C. Mealli, Inorg. Chem., 17 (1978) 1323–1329.
[5] M. Mohan, S.M. Holmes, R.J. Butcher, J.P. Jasinski and C.J. Carrano, Inorg. Chem., 31 (1992) 2029–2034.
[6] E. Kime-Hunt, K. Spartalian, M. DeRusha, C.M. Nunn and C.J. Carrano, Inorg. Chem., 28 (1989) 4392–4399.
[7] M. Mohan, M.R. Bond, T. Otieno and C.J. Carrano, Inorg. Chem., 34 (1995) 1233–1242.
[8] C.J. Carrano, M. Mohan, S.M. Holmes, R. de la Rosa, A. Butler, J.M. Charnock and C.D. Garner, Inorg. Chem., 33 (1994) 646–655.
[9] P. Burchill and M.G.H. Wallbridge, Inorg. Nucl. Chem. Lett., 12 (1976) 93–97.
[10] J. Sundermeyer, J. Putterlik, M. Foth, J.S. Field and N. Ramesar, Chem. Ber., 127 (1994) 1201–1212.
[11] A. Butler and C.J. Carrano, Coord. Chem. Rev., 109 (1991) 61–105.
[12] D. Rehder, Angew. Chem., Int. Ed. Engl., 30 (1991) 148–167.
[13] R. Wever and K. Kustin, Adv. Inorg. Chem., 35 (1990) 81–115.
[14] A. Butler and J.V. Walker, Chem. Rev., 93 (1993) 1937–1944.
[15] H. Vilter and D. Rehder, Inorg. Chim. Acta, 136 (1987) L7–L10.
[16] D. Rehder, W. Priebsch and M. Oeynhausen, Angew. Chem. Int. Ed. Engl., 28 (1989) 1221–1222.
[17] M.G.M. Tromp, G. Olafson, B.E. Krenn and R. Wever, Biochim. Biophys. Acta, 1040 (1990) 192–198.
[18] (a) J.M. Arber, E. de Boer, C.D. Garner, S.S. Hasnian and R. Wever, Biochemistry, 28 (1989) 7968–7973; (b) E. de Boer, Y. van Kooyk, M.G.M. Tromp, H. Plat and R. Wever, Biochim. Biophys. Acta, 869 (1986) 48–53.
[19] E. de Boer, K. Boon and R. Wever, Biochemistry, 27 (1988) 1629–1635.
[20] D. Collison, D.R. Eardley, F.E. Mabbs, A.K. Powell and S.S. Turner, Inorg. Chem., 32 (1993) 664–671.
[21] R.L. Beddoes, D. Collison, F.E. Mabbs and M.A. Passand, Polyhedron, 9 (1990) 2483–2489.
[22] D. Collison, F.E. Mabbs, M.S. Passand, K. Rigby and W.E. Cleland, Polyhedron, 8 (1989) 1827–1829.
[23] D. Collison, F.E. Mabbs and K. Rigby, Polyhedron, 8 (1989) 1830–1832.
[24] N.E. Heimer and W.E. Cleland, Acta Crystall., C46 (1990) 2049–2051.
[25] S. Holmes and C.J. Carrano, Inorg. Chem., 30 (1991) 1231–1235.
[26] S. Trofimenko, J.C. Calabrese and J.S. Thompson, Inorg. Chem., 26 (1987) 1508–1514.

[27] D. Rehder, C. Weidemann, A. Duch and W. Priebsch, Inorg. Chem., 27 (1988) 584–587.
[28] (a) M. Koppen, G. Fresen, K. Wieghardt, R.M. Llusar, B. Nuber and J. Weiss, Inorg. Chem., 27 (1988) 721–727; (b) P. Knopp, K. Wieghardt, B. Nuber, J. Weiss and W.S. Sheldrick, Inorg. Chem., 29 (1990) 363–371.
[29] C.J. Carrano, R. Verastgue and M.R. Bond, Inorg. Chem., 31 (1993) 3589–3590.
[30] (a) P. Knopp and K. Wieghardt, Inorg. Chem., 30 (1991) 4061–4066; (b) R. Hotzelmann and K. Weighardt, Inorg. Chem., 32 (1993) 114–116.
[31] R. Hotzelmann, K. Wieghardt, U. Flörke, H.J. Haupt, D.C. Weatherburn, J. Bonvoisin, G. Blondin and J.J. Girerd, J. Am. Chem. Soc., 114 (1992) 1681–1696.
[32] (a) C. Santini-Scampucci and G. Wilkinson, J. Chem. Soc. Dalton Trans. (1976) 807–811; (b) D.H. Williamson, C. Santini-Scampucci and G. Wilkinson, J. Organomet. Chem., 77 (1974) C25–C26.
[33] D.L. Reger, C.A. Swift and L. Lebioda, J. Am. Chem. Soc., 105 (1983) 5343–5347.
[34] J. Fernandez-Baeza, F.A. Jalon, A. Otero and M.A. Rodrigo-Blanco, J. Chem. Soc. Dalton Trans. (1995) 1015–1021.
[35] L.G. Hubert-Pfalzgraf and J.G. Riess, Inorg. Chim. Acta, 47 (1980) 7–11.
[36] L.G. Hubert-Pfalzgraf and M. Tsunoda, Polyhedron, 2 (1983) 203–210.
[37] D.C. Bradley, M.B. Hursthouse, J. Newton and N.P.C. Walker, J. Chem. Soc. Chem. Commun. (1984) 188–190.
[38] D.L. Reger, C.A. Swift and L. Lebioda, Inorg. Chem., 23 (1984) 349–354.
[39] F. Bottomley and S. Karslioglou, Organometallics, 11 (1992) 326–337.
[40] (a) V.C. Gibson and T.P. Kee, J. Chem. Soc. Chem. Commun. (1989) 656–657; (b) V.C. Gibson, T.P. Kee and W. Clegg, J. Chem. Soc. Dalton Trans. (1990) 3199–3210.
[41] W.A. Nugent and J.M. Mayer, Metal–Ligand Multiple Bonds, Wiley, New York, NY, 1988.
[42] D.E. Wigley, Prog. Inorg. Chem., 42 (1994) 239–482.
[43] W.A. Nugent, R.J. McKinney, R.V. Kasowski and F.A. Van Catledge, Inorg. Chim. Acta, 65 (1982) L91–L93.
[44] D.N. Williams, J.P. Mitchell, A.D. Poole, U. Siemeling, W. Clegg, D.C.R. Hockless, P.A. O'Neil and V.C. Gibson, J. Chem. Soc. Dalton Trans. (1992) 739–751.
[45] S. Schmidt and J. Sundermeyer, J. Organomet. Chem., 472 (1994) 127–138.
[46] F. Biasotto and M. Etienne, unpublished results, 1994.
[47] J.L. Templeton, Adv. Organomet. Chem., 29 (1989) 1–100.
[48] M.J. McGeary, A.S. Gamble and J.L. Templeton, Organometallics, 7 (1988) 271–279.
[49] M. Etienne, P.S. White and J.L. Templeton, Organometallics, 10 (1991) 3801–3803.
[50] M. Etienne, unpublished results, 1995.
[51] M. Etienne, B. Donnadieu, J. Fernandez-Baeza, F. Jalon, A. Otero and M.E. Rodrigo-Blanco, in preparation.
[52] G. Smith, R.R. Schrock, M.R. Churchill and W.J. Youngs, Inorg. Chem., 20 (1981) 387–393.
[53] M.D. Curtis, J. Real and D. Kwon, Organometallics, 8 (1989) 1644–1651.
[54] (a) S.J. McLain, R.R. Schrock, P.R. Sharp, M.R. Churchill and W.J. Youngs, J. Am. Chem. Soc., 101 (1979) 263–265; (b) M.R. Churchill and W.J. Youngs, Inorg. Chem., 18 (1979) 1697–1702.
[55] M. Etienne, unpublished work.
[56] M. Bovens, T. Gerfin, V. Gramlich, W. Petter, L.M. Venanzi, M.T. Haward, S.A. Jackson and O. Eisenstein, New J. Chem., 16 (1992) 337–345.
[57] J.L. Templeton, J.L. Caldarelli, S.G. Feng, C.C. Philipp, M.B. Wells, R.E. Woodworth and P.S. White, J. Organomet. Chem., 478 (1994) 103–110.
[58] J.L. Templeton and B.C. Ward, J. Am. Chem. Soc., 102 (1980) 3288–3290.
[59] A. Antinolo, P. Gomez-Sal, J. Martinez de Varduya, A. Otero, P. Royo, S. Martinez Carrera and S. Garcia Blanco, J. Chem. Soc. Dalton Trans. (1987) 975–980.
[60] M. Etienne, P. Zeline, J.L. Templeton and P.S. White, New. J. Chem., 17 (1993) 515–517.
[61] P.L. Watson and R.G. Bergman, J. Am. Chem. Soc., 102 (1980) 2698–2703.
[62] F.J. Feher, M. Green and R. Rodrigues, J. Chem. Soc. Chem. Commun. (1987) 1206–1208.
[63] A.S. Gamble, K.R. Birdwhistell and J.L. Templeton, J. Am. Chem. Soc., 112 (1990) 1818–1824.
[64] M.A. Collins, S.G. Feng, P.S. White and J.L. Templeton, J. Am. Chem. Soc., 114 (1992) 3771–3775.
[65] M. Etienne, P.S. White and J.L. Templeton, Organometallics, 12 (1993) 4010–4015.

[66] M. Brookhart and M.L.H. Green, J. Organomet. Chem., 250 (1983) 395–408.
[67] M. Brookhart, M.L.H. Green and L.-L. Wong, Prog. Inorg. Chem., 36 (1988) 1–124.
[68] M. Etienne, Organometallics, 13 (1994) 410–412.
[69] M. Etienne, F. Biasotto and R. Mathieu, J. Chem. Soc. Chem. Commun. (1994) 1661–1662.
[70] M. Etienne, unpublished results.
[71] L.J. Guggenberger, P. Meakin and F.N. Tebbe, J. Am. Chem. Soc., 96 (1974) 5420–5427.
[72] H. Yasuda, H. Yamamoto, T. Arai, A. Nakamura, J. Chen, Y. Kai and N. Kasai, Organometalllics, 10 (1991) 4058–4066.
[73] A.D. Poole, D.N. Williams, A.M. Kenwright, V.C. Gibson, W. Clegg, D.C.R. Hockless and P.A. O'Neil, Organometallics, 12 (1993) 2549–2555.
[74] Z. Guo, D.C. Swenson and R.G. Jordan, Organometallics, 13 (1994) 1424–1432.
[75] R.R. Schrock, Acc. Chem. Res., 12 (1979) 98–104.
[76] J.D. Fellman, R.R. Schrock and D.D. Traficante, Organometallics, 1 (1982) 481–484.
[77] M.D. Curtis, J. Real, W. Hirpo and W.M. Butler, Organometallics, 9 (1990) 66–74.
[78] W. Hirpo and M.D. Curtis, Organometallics, 13 (1994) 2706–2712.
[79] D.S. Williams and R.R. Schrock, Organometallics, 12 (1993) 1148–1160.
[80] V.C. Gibson, J. Chem. Soc. Dalton Trans. (1994) 1607–1618.
[81] A.D. Poole, V.C. Gibson and W. Clegg, J. Chem. Soc. Chem. Commun. (1992) 237–239.
[82] M. Etienne, unpublished results, 1995.
[83] (a) W.E. Piers and J.E. Bercaw, J. Am. Chem. Soc., 112 (1990) 9406–9407; (b) H. Krauledat and H.-H. Brintzinger, Angew. Chem. Int. Ed. Engl., 29 (1990) 1412–1413; (c) N.S. Barta, B.A. Kirk and J.R. Stille, J. Am. Chem. Soc., 116 (1994) 8912–8919.
[84] M. Etienne and F. Biasotto, unpublished results, 1995.
[85] F. Biasotto, M. Etienne and F. Dahan, Organometallics, 14 (1995) 1870–1874.
[86] L. Carlton, J.L. Davidson, P. Ewing, L. Manojlovic-Muir and K.W. Muir, J. Chem. Soc. Chem. Commun. (1985) 1474–1476.
[87] (a) C.G. Conole, M. Green, M. McPartlin, C. Reeve and C.M. Woolhouse, J. Chem. Soc. Chem. Commun. (1988) 1310–1313; (b) M. Green, M.F. Mahon, K.C. Molloy, C.B.M. Nation and C.M. Woolhouse, J. Chem. Soc. Chem. Commun. (1991) 1587–1588.
[88] (a) J.R. Morrow, T.L. Tonker and J.L. Templeton, J. Am. Chem. Soc., 107 (1985) 5004–5005; (b) S.G. Feng, A.S. Gamble and J.L. Templeton, Organometallics, 8 (1989) 2024–2031.
[89] W. Hirpo and M.D. Curtis, J. Am. Chem. Soc., 110 (1988) 5218–5219.
[90] C.E. Kriley, J.L.Kerschner, P.E. Fanwick and I.P. Rothwell, Organometallics, 12 (1993) 2051–2058.
[91] B. Hessen, A. Meetsma, F. van Bolhuis, J.H. Teuben, G. Helgesson and S. Jagner, Organometallics, 9 (1990) 1925–1936.
[92] M.R. Bond, L.M. Mokry, T. Otieno, J. Thompson and C.J. Carrano, Inorg. Chem., 34 (1995) 1894–1905.
[93] L.M. Mokry, J. Thompson, M.R. Bond, T. Otieno, M. Mohan and C.J. Carrano, Inorg. Chem., 33 (1994) 2705–2706.
[94] P. Lorente and M. Etienne, unpublished results.
[95] (a) A.N. Nesmeyanov, K.N. Anisimov, N.E. Kolobova and A.A. Pasynskii, Izv. Akad. Nauk SSSR Ser. Khim. (1969) 100; (b) B.E.R. Schilling, R. Hoffmann and D.L. Lichtenberger, J. Am. Chem. Soc., 101 (1979) 585–591.
[96] A.N. Nesmeyanov, A.I. Gusev, A.A. Pasynskii, K.N. Anisimov, N.E. Kolobova and Yu.T. Struchkov, J. Chem. Soc. Chem. Commun. (1969) 277–278.
[97] S. Scheuer, J. Fischer and J. Kress, Organometallics, 14 (1995) 2627–2629.